

# The DMT Dynamical Model for Electromagnetic Production of Pions

Shin Nan Yang  
National Taiwan University

Collaborators: S. S. Kamalov (Dubna)  
D. Drechsel, L. Tiator (Mainz)  
Guan Yeu Chen (Taipei)

## DMT dynamical model

---

“New Theoretical Tools for Nucleon Resonance Analysis” Workshop,  
Aug. 29 – September 2, 2005, Argonne National Laboratory, USA

# Outline

- Motivation
- Meson-exchange  $\pi N$  model below 400 MeV
- DMT dynamical model for pion e.m. production
- Extension to higher energies
- Conclusions

# Motivation

QCD  $\longleftrightarrow$  Hadronic phenomena

- low energies — ChPT
- high energies, high momentum transfer — pQCD
- medium energies
  - LQCD
  - Phenomenology : hadron models, reaction theory

Aim: To construct a coupled-channel dynamical model to study  $\pi N$  scattering and pion e.m. production



- low energies:  
e.m. threshold pion production, low energy theorems and compare with ChPT
- medium energies:  
N! $\Delta$  transition form factors, resonance parameters
- high energy and high momentum transfer:  
transition to pQCD region?

# Threshold $\pi^0$ electromagnetic production

## Photoproduction

|                                  | HBCChPT $O(p^4)$ | Dispersion relation | Exp. ( $10^{-3}/m_\pi$ )  |
|----------------------------------|------------------|---------------------|---------------------------|
| $E_{0^+} \left  \pi^0 p \right.$ | -1.1             | -1.22               | $-1.33 \pm 0.88 \pm 0.03$ |
| $E_{0^+} \left  \pi^+ n \right.$ | -0.43            | -0.56               | $-0.45 \pm 0.06 \pm 0.02$ |

- LET (Gauge Inv. + PCAC)  $\square E_{0^+}(\pi^0 p) = -2.3 \times 10^{-3}/m_\pi$

$$E_{0^+}(\pi^0 p) = -\frac{2.3 \times 10^{-3}}{m_\pi} (1 + O(\mu))$$

ChPT; The above expansion in  $\mu = m_\pi/m_N$  converges slowly

## Electroproduction

HBChPT □ a low energy effective field theory  
respecting the symmetries of QCD, in  
particular, **chiral** symmetry  
perturbative calculation □ crossing symmetric

DMT □ Lippman-Schwinger type formulation with  
potential constructed from **chiral** effective  
lagrangian  
unitarity □ loops to all orders

**What are the predictions of DMT?**

# $\gamma^* N \leftrightarrow \Delta$ transition

---

- In a symmetric SU(6) quark model, the e.m. excitation of the  $\Delta$  could proceed only via M1 transition
- If the  $\Delta$  is deformed, then the photon can excite a nucleon into a  $\Delta$  through electric E2 and Coulomb C2 quadrupole transitions
- At  $Q^2 = 0$ , recent experiments give,  
 $R_{EM} = E2/M1 \approx -2.5\%$ ,  
( $Q_{N|\Delta} = -0.108 \text{ fm}^2 < 0$ , oblate),

indication of a deformed  $\Delta$

# Resonance parameters

For example, in the case of the four-star resonance  $S_{11}(1535)$ ,

- Breit-Wigner mass (MeV): 1520 – 1555 ( $\frac{1}{4}$  1535)
- Breit-Wigner width (MeV): 100 – 200 ( $\frac{1}{4}$  150)
  - 120  $\pm$  20, Hoehler '79 ( $\pi N ! \pi N$ )
  - 270  $\pm$  50, Cutkovsky, '79 ( $\pi N ! \pi N$ )
  - 66, Arndt '95 ( $\pi N ! \pi N$ )
  - 151  $\pm$  27, Manley '92 ( $\pi N ! \pi N, \pi\pi N$ )
  - 151 – 198, Mosel '98 ( $\pi N ! \pi N, \pi\pi N, \eta N, K\Sigma$ )
- Pole position: (1495-1515, 90-250)
- $A_{1/2}^p(10^{-3} \text{ GeV}^{-1/2})$ :
  - 60, Arndt '96 ( $\gamma N ! \pi N$ )
  - 120, Krusche '97 ( $\gamma N ! \eta N$ )

Simultaneous analysis of  
( $\pi N ! \pi N, \gamma N ! \pi N, \gamma N ! \eta N$ )



# $\gamma^* N \leftrightarrow \Delta$ transition and pQCD

pQCD predicts that as  $Q^2 \rightarrow 1$ ,

- hadronic helicity conservation:  $A_{1/2} \rightarrow A_{3/2}$
- scaling:  $A_{1/2}^\Delta : Q^{-3}$ ,  $A_{3/2}^\Delta : Q^{-5}$ ,  $S_{1/2}^\Delta : Q^{-3}$



$$R_{EM} = E_{1+}^{(3/2)} / M_{1+}^{(3/2)} \rightarrow 1,$$

$$R_{SM} = S_{1+}^{(3/2)} / M_{1+}^{(3/2)} \rightarrow \text{const.}$$

What region of  $Q^2$  corresponds to the transition from nonperturbative to pQCD description?

# Meson-exchange $\pi$ N model below 400 MeV

---

Bethe-Salpeter equation

$$T_{\pi N} = B_{\pi N} + B_{\pi N} G_0 T_{\pi N},$$

where

$B_{\pi N}$  = sum of all irreducible two-particle Feynman amplitudes

$G_0$  = relativistic free pion-nucleon propagator

can be rewritten as  $\Rightarrow$

$$T_{\pi N} = \mathcal{B}_{\pi N} + \mathcal{B}_{\pi N} \mathcal{G}_0 T_{\pi N},$$

with

$$\mathcal{B}_{\pi N} = B_{\pi N} + B_{\pi N} (G_0 - \mathcal{G}_0) \mathcal{B}_{\pi N}.$$

# Three-dimensional reduction

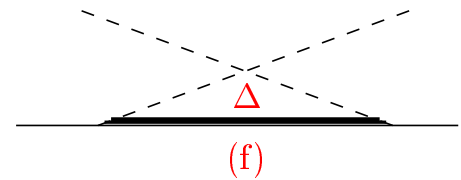
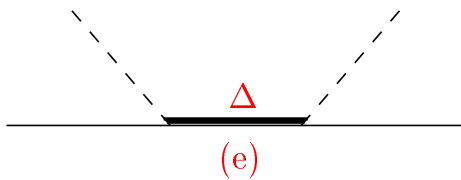
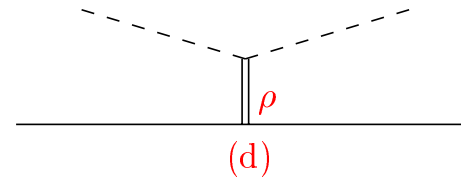
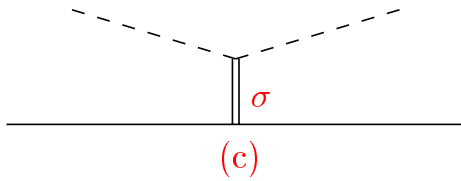
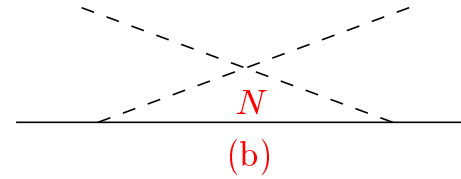
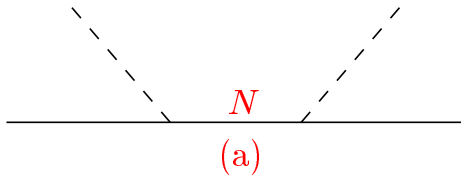
---

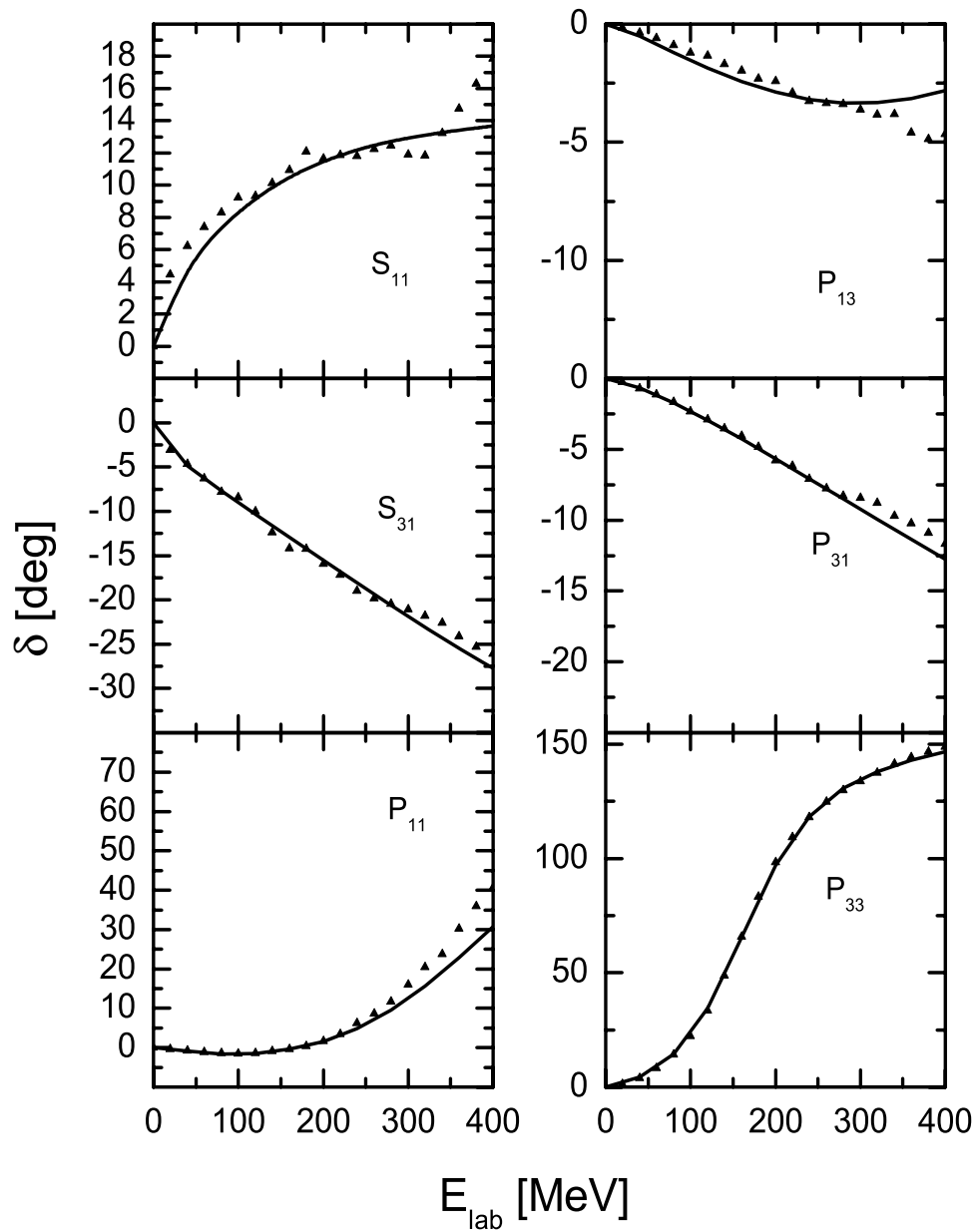
Choose a  $\mathcal{G}_0(k, P)$  such that

1.  $T_{\pi N} = \mathcal{B}_{\pi N} + \mathcal{B}_{\pi N} \mathcal{G}_0 T_{\pi N}$  becomes  
three-dimensional
2.  $\mathcal{G}_0$  can reproduce  $\pi N$  elastic cut

Cooper-Jennings reduction scheme

Choose  $\mathcal{B}_{\pi N}$  to be given by





# Dynamical model for $\gamma N \rightarrow \pi N$

To order  $e$ , the t-matrix for  $\gamma N \rightarrow \pi N$  is written as

$$t_{\gamma\pi}(E) = v_{\gamma\pi} + \sum_{\kappa} v_{\gamma\kappa} g_{\kappa}(E) t_{\kappa N}(E), \quad (1)$$

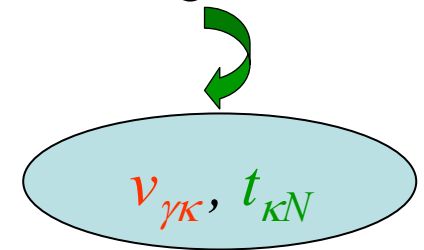
where,

$v_{\gamma\kappa}$  = transition potential,

$t_{\kappa N}(E)$  =  $\kappa N$  t-matrix,

$$g_{\kappa}(E) = \frac{1}{E - H_0}.$$

two ingredients



Multipole decomposition of (1) gives the physical amplitude in channel  $\alpha = (\xi, l_{\pi}, j)$ , (with  $\eta N$  intermediate states neglected)

$$t_{\gamma\pi}^{(\alpha)}(q_E, k; E + i\varepsilon) = \exp(i\delta^{(\alpha)}) \cos \delta^{(\alpha)}$$

Off-shell

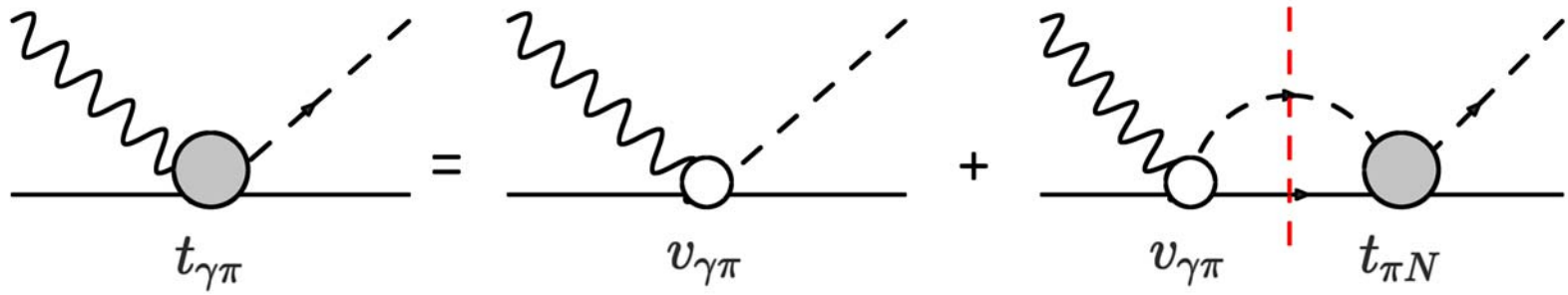
$$\times \left[ v_{\gamma\pi}^{(\alpha)}(q_E, k) + P \int_0^{\infty} dq' \frac{q'^2 R_{\pi N}^{(\alpha)}(q_E, q'; E) v_{\gamma\pi}^{(\alpha)}(q', k)}{E - E_{\pi N}(q')} \right]$$

where

$\delta^{(\alpha)}, R^{(\alpha)}$  :  $\pi N$  scattering phase shift and reaction matrix in channel  $\alpha$

$k = |k|, q_E$  : photon and pion on-shell momentum

**Both on- & off-shell**



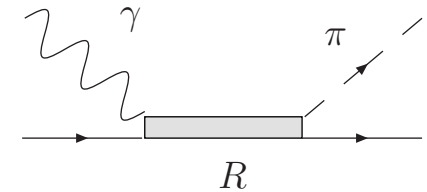
If the transition potential  $v_{\gamma\pi}$  consists of two terms,

$$v_{\gamma\pi}(E) = v_{\gamma\pi}^B(E) + v_{\gamma\pi}^R(E),$$

where

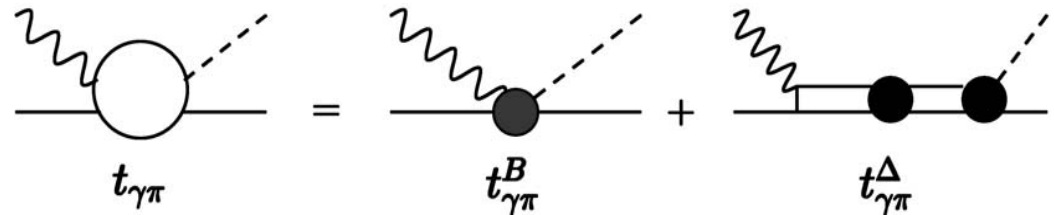
$v_{\gamma\pi}^B$  = background transition potential

$v_{\gamma\pi}^R$  = contribution of a bare resonance  $R$



then one obtains

$$t_{\gamma\pi}(E) = t_{\gamma\pi}^B(E) + t_{\gamma\pi}^R(E),$$



with

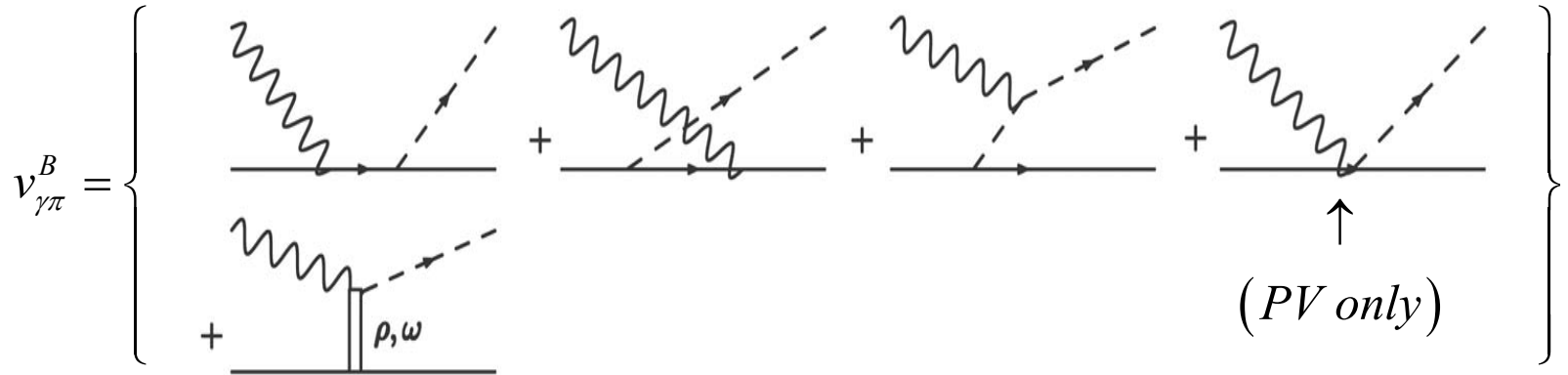
$$t_{\gamma\pi}^B(E) = v_{\gamma\pi}^B + \sum_k v_{\gamma k}^B g_k(E) t_{k\pi}(E)$$

$$t_{\gamma\pi}^R(E) = v_{\gamma\pi}^R + \sum_k v_{\gamma k}^R g_k(E) t_{k\pi}(E)$$

both  $t^B$  and  $t^R$  satisfy  
Fermi-Watson theorem,  
respectively.



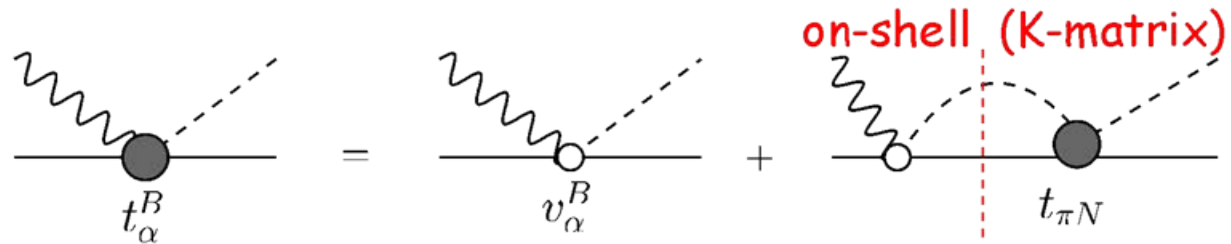
# DMT Model



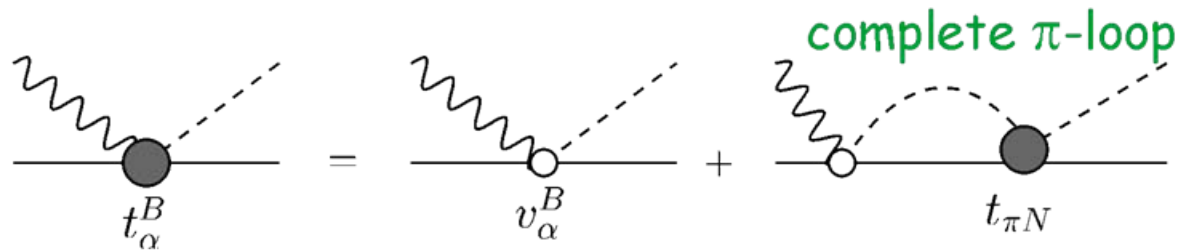
$$t_{\gamma\pi}^{B,\alpha} = \exp(i\delta^{(\alpha)}) \cos \delta^{(\alpha)} \begin{cases} v_{\gamma\pi}^{B,\alpha}(W, Q^2) + P \int_0^\infty dq' \frac{q'^2 R_{\pi N}^{(\alpha)}(q_E, q'; E) v_{\gamma\pi}^{B,\alpha}(q', k)}{E - E_{\pi N}(q')}, & DM \\ v_{\gamma\pi}^{B,\alpha}(W, Q^2), & MAID \end{cases}$$

in the dynamical approach the background is differently defined:

**K-matrix:**  
(MAID/SAID)



**dynamical approach:**

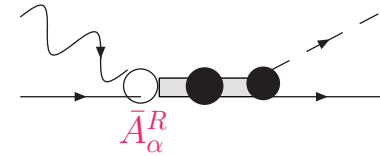


$$t_{\alpha}^B(DM) = v_{\alpha}^B e^{i\delta_{\alpha}} \cos \delta_{\alpha} + P \int_0^{\infty} dq' \frac{q'^2 t_{\pi N}^{(\alpha)}(q_E, q') v_{\alpha}^B(q')}{E - E_{\pi N}(q')}$$

additional contribution from  
explicit  $\pi$ -loop integration

In DMT, we approximate the resonance contribution  $A_\alpha^R(W, Q^2)$  by the following Breit-Winger form

$$A_\alpha^R(W, Q^2) = \bar{A}_\alpha^R(Q^2) \frac{f_{\gamma R}(W) \Gamma_R M_R f_{\pi R}(W)}{M_R^2 - W^2 - i M_R \Gamma_R} e^{i\phi},$$



with

$f_{\pi R}$  = Breit-Winger factor describing the decay of the resonance R

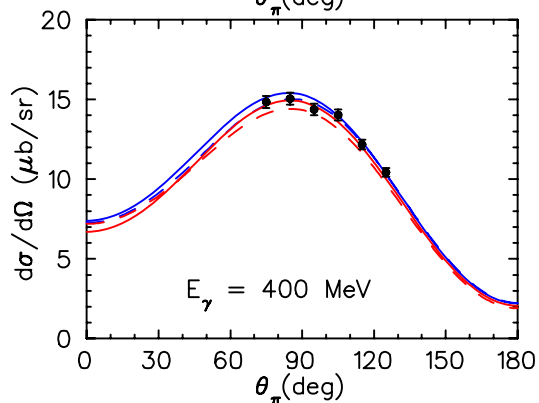
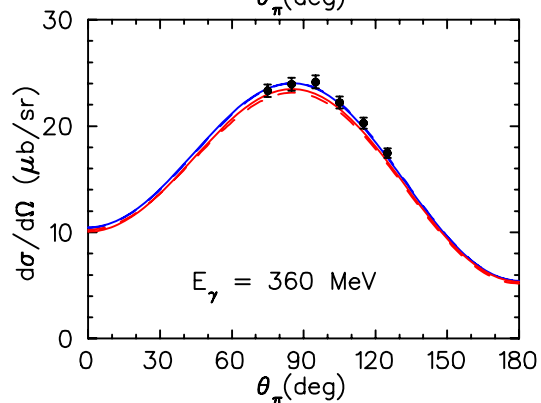
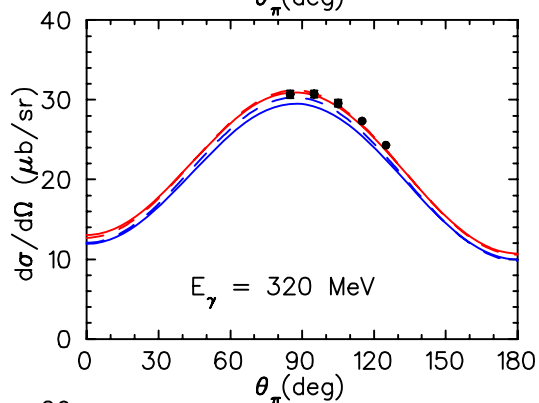
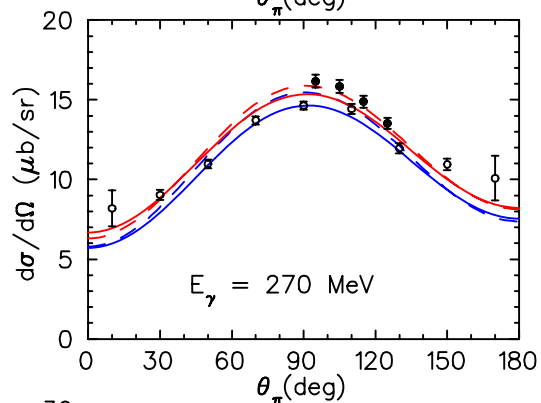
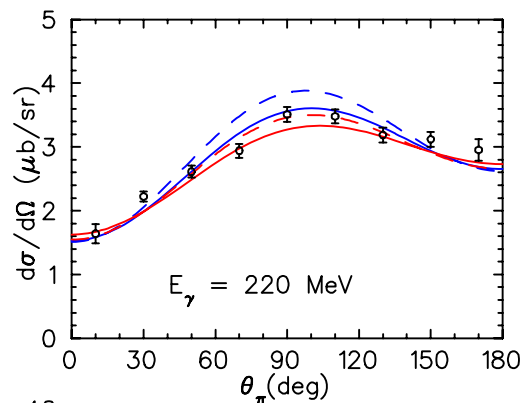
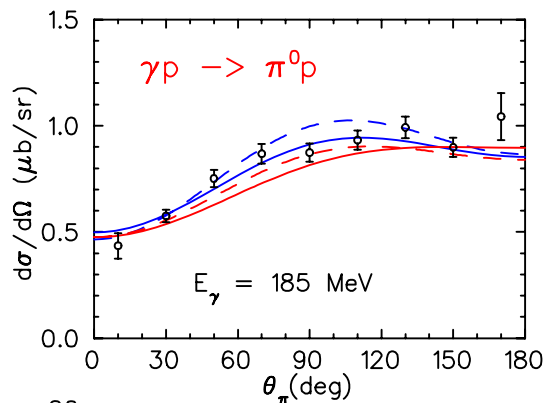
$\Gamma_R(W)$  = total width

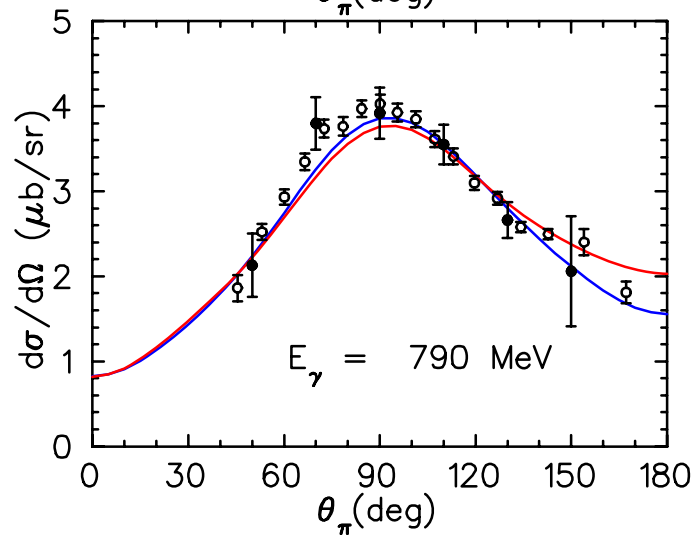
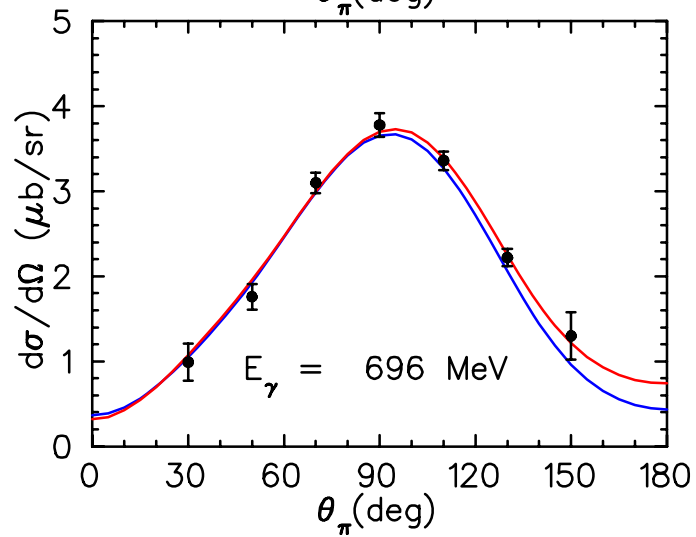
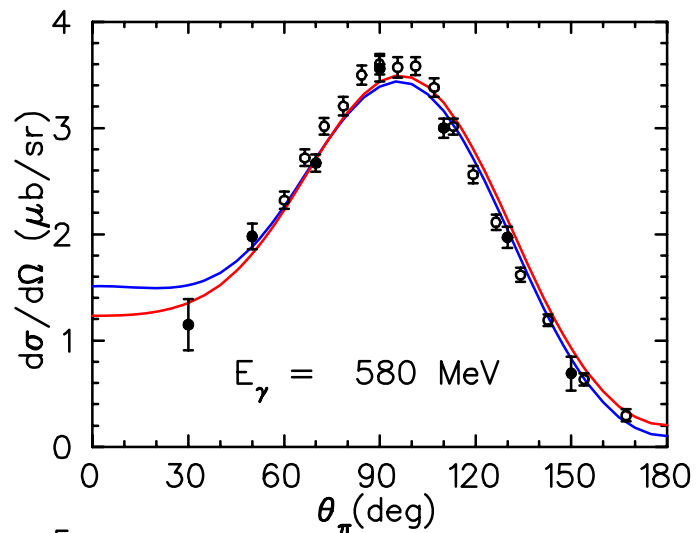
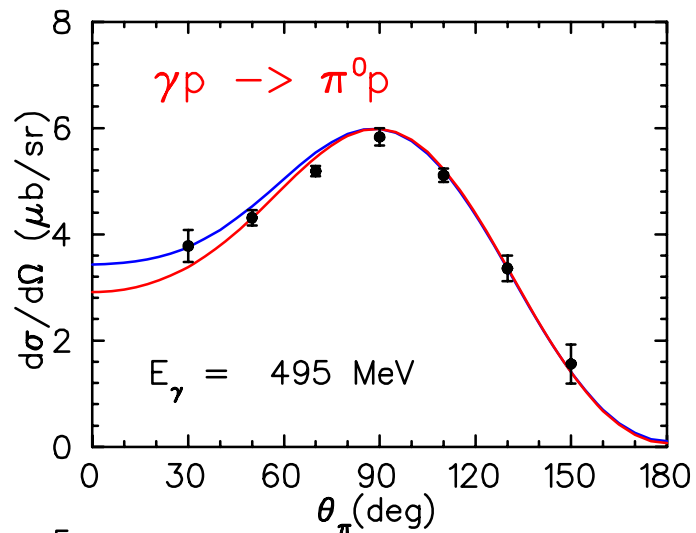
$M_R$  = physical mass

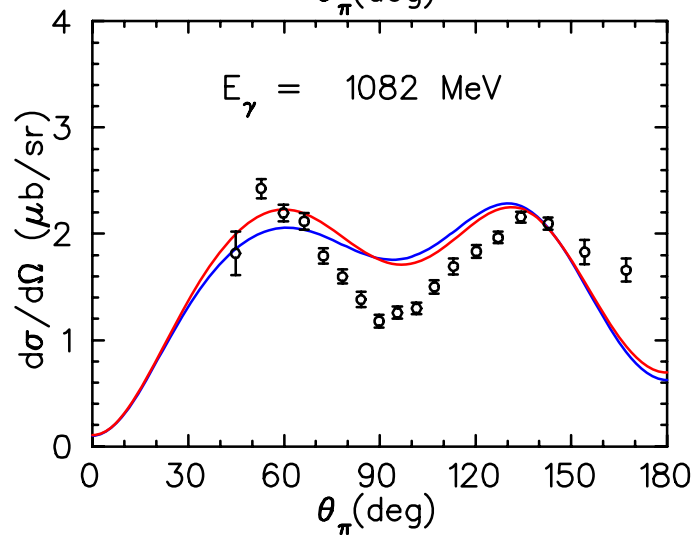
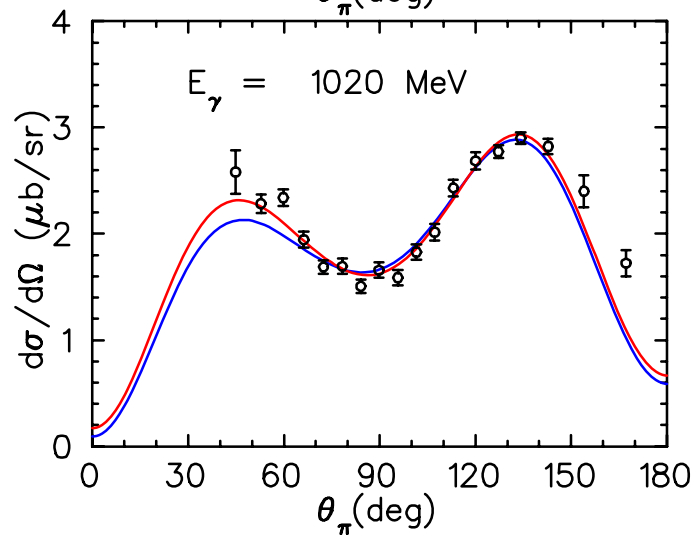
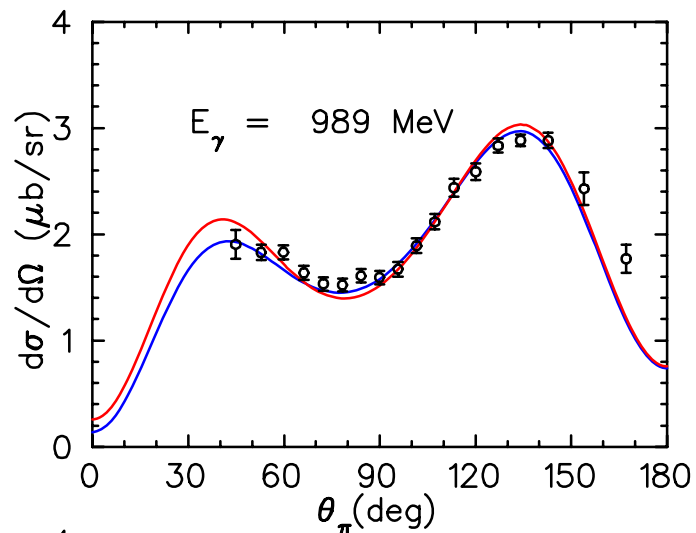
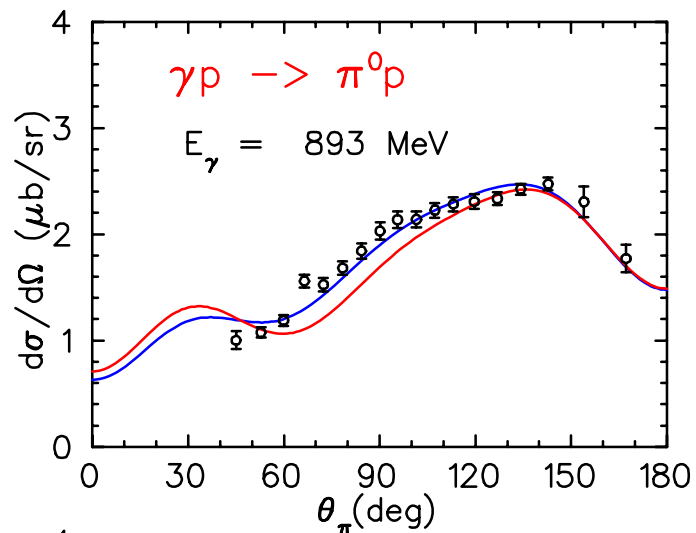
$\phi(W)$  = to adjust the phase of the total multipole to be equal to the corresponding  $\pi N$  phase shift  $\delta^{(\alpha)}$ .

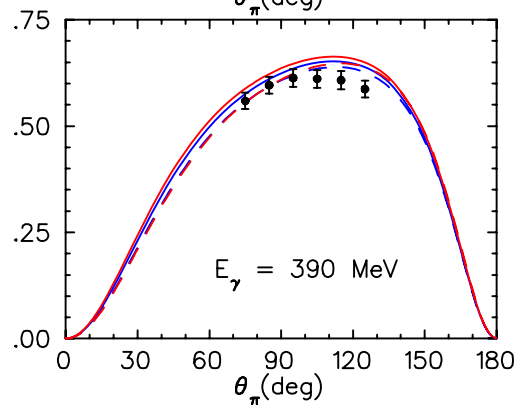
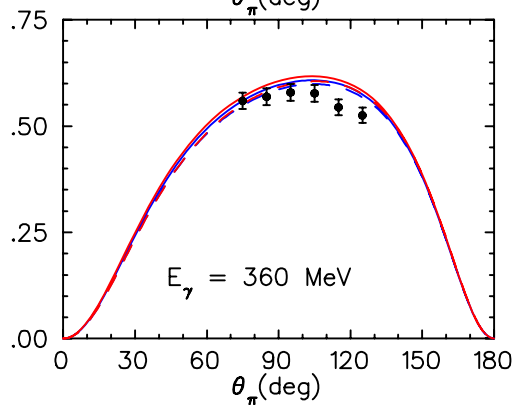
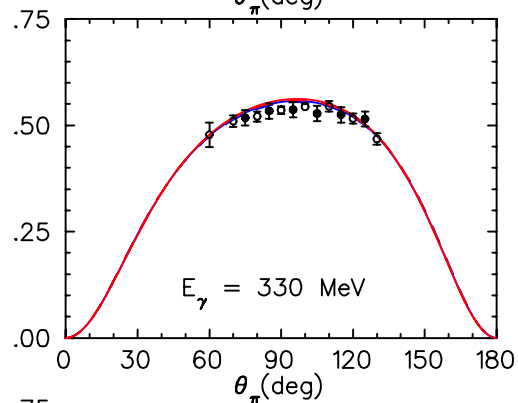
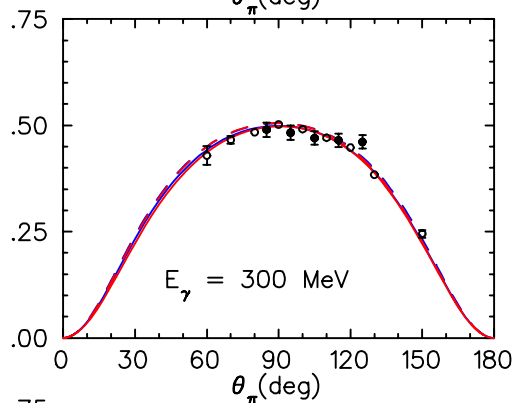
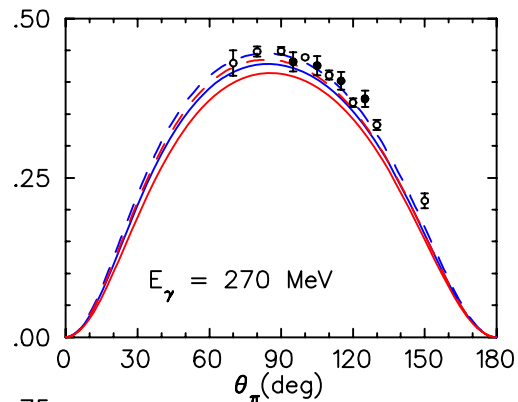
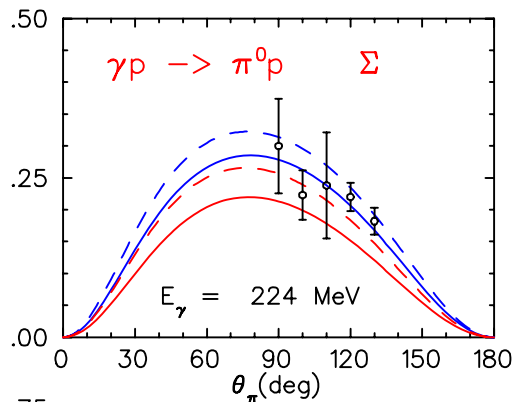
Note that  $\bar{A}_\alpha^R(Q^2) = \begin{cases} \text{bare, DMT} \\ \text{dressed, MAID} \end{cases}$

— MAID  
— DMT

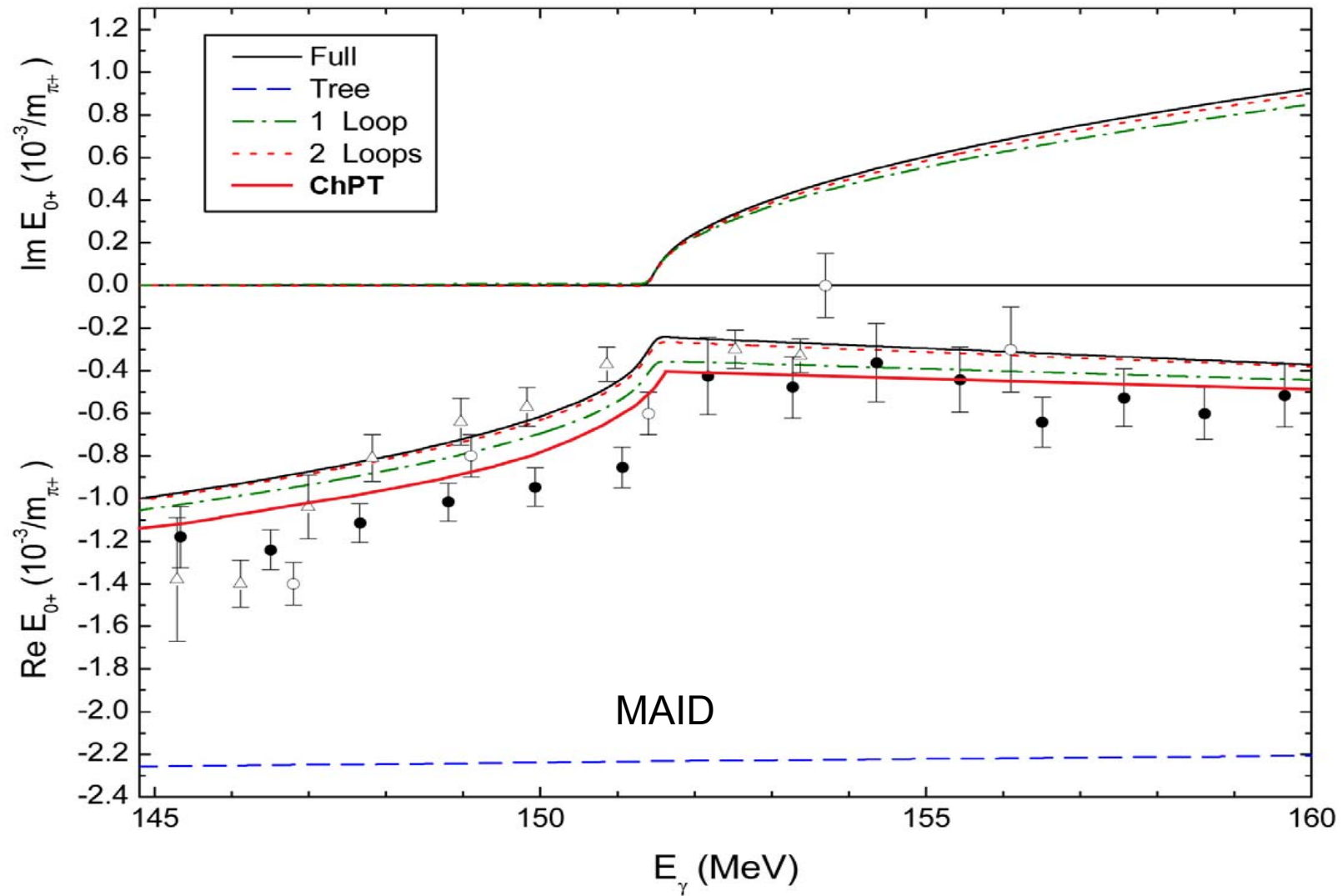








$$\gamma p \rightarrow \pi^0 p$$





Threshold values of  $E_{0+}$  (in units of  $10^{-3}/m_\pi$ ) for different channels predicted by DMT ( $Q^2 = 0$ )

|                 | Tree   | 1-loop           | 2-loop           | Full   | ChPT            | Exp.             |
|-----------------|--------|------------------|------------------|--------|-----------------|------------------|
| $\pi \square p$ | -2.26  | -1.06<br>(53.1%) | -1.01<br>(2.2%)  | -1.00  | -1.1            | $-1.33 \pm 0.11$ |
| $\pi \square n$ | 27.72  | 28.62<br>(3.2%)  | 28.82<br>(0.7%)  | 28.85  | $28.2 \pm 0.6$  | $28.3 \pm 0.3$   |
| $\pi \square n$ | 0.46   | 2.09<br>(354.3%) | 2.15<br>(13.0%)  | 2.18   | 2.13            |                  |
| $\pi \square p$ | -31.65 | -32.98<br>(4.2%) | -33.27<br>(0.9%) | -33.31 | $-32.7 \pm 0.6$ | $-31.8 \pm 1.9$  |

|                   | DMT                 | HBCChPT      |
|-------------------|---------------------|--------------|
| chiral symmetry   | yes                 | yes          |
| crossing symmetry | no                  | yes          |
| unitarity         | yes                 | no           |
| counting          | loop( $g_{\pi N}$ ) | chiral power |

Threshold values of  $E_{0+} (10^{-3}/m_\pi)$  at  $Q^2 = 0.05(\text{GeV}/c)^2$  for  
different channels predicted by DMT

|                 | Tree   | 1-loop | 2-loop | Full        | ChPT        | Exp.             |
|-----------------|--------|--------|--------|-------------|-------------|------------------|
| $\pi \square p$ | -0.19  | 0.96   | 1.02   | <b>1.03</b> | <b>0.27</b> | <b>0.57±0.11</b> |
| $\pi \square n$ | 23.92  | 24.86  | 25.09  | 25.12       |             |                  |
| $\pi \square n$ | 1.53   | 3.00   | 3.07   | 3.09        |             |                  |
| $\pi \square p$ | -26.42 | -27.69 | -27.96 | -28.00      |             |                  |

Threshold values of  $E_{0+} (10^{-3}/m_\pi)$  at  $Q^2 = 0.1(\text{GeV}/c)^2$  for  
different channels predicted by DMT

|                 | Tree   | 1-loop | 2-loop | Full        | ChPT        | Exp.             |
|-----------------|--------|--------|--------|-------------|-------------|------------------|
| $\pi \square p$ | 1.30   | 2.37   | 2.43   | <b>2.44</b> | <b>1.42</b> | <b>0.58±0.18</b> |
| $\pi \square n$ | 20.89  | 21.88  | 22.10  | 22.13       |             |                  |
| $\pi \square n$ | 2.27   | 3.57   | 3.64   | 3.66        |             |                  |
| $\pi \square p$ | -22.33 | -23.51 | -23.75 | -23.79      |             |                  |

Threshold values of  $L_{0+}$  ( $10^{-3}/m_\pi$ ) at  $Q^2 = 0.05(\text{GeV}/c)^2$  for  
different channels predicted by DMT

|                 | Tree  | 1-loop | 2-loop | Full         | ChPT         | Exp.             |
|-----------------|-------|--------|--------|--------------|--------------|------------------|
| $\pi \square p$ | -1.97 | -16.7  | -1.67  | <b>-1.67</b> | <b>-1.55</b> | -                |
| $\pi \square n$ | 4.96  | 5.06   | 5.10   | 5.11         |              | <b>1.29±0.02</b> |
| $\pi \square n$ | 0.05  | 0.54   | 0.56   | 0.57         |              |                  |
| $\pi \square p$ | -7.92 | -8.33  | -8.42  | -8.43        |              |                  |

Threshold values of  $L_{0+}$  ( $10^{-3}/m_\pi$ ) at  $Q^2 = 0.1(\text{GeV}/c)^2$  for  
different channels predicted by DMT

|                 | Tree  | 1-loop | 2-loop | Full         | ChPT         | Exp.             |
|-----------------|-------|--------|--------|--------------|--------------|------------------|
| $\pi \square p$ | -1.32 | -1.15  | -1.15  | <b>-1.15</b> | <b>-1.33</b> | -                |
| $\pi \square n$ | 2.32  | 2.35   | 2.37   | 2.38         |              | <b>1.38±0.01</b> |
| $\pi \square n$ | 0.06  | 0.36   | 0.37   | 0.37         |              |                  |
| $\pi \square p$ | -4.37 | -4.61  | -4.66  | -4.67        |              |                  |

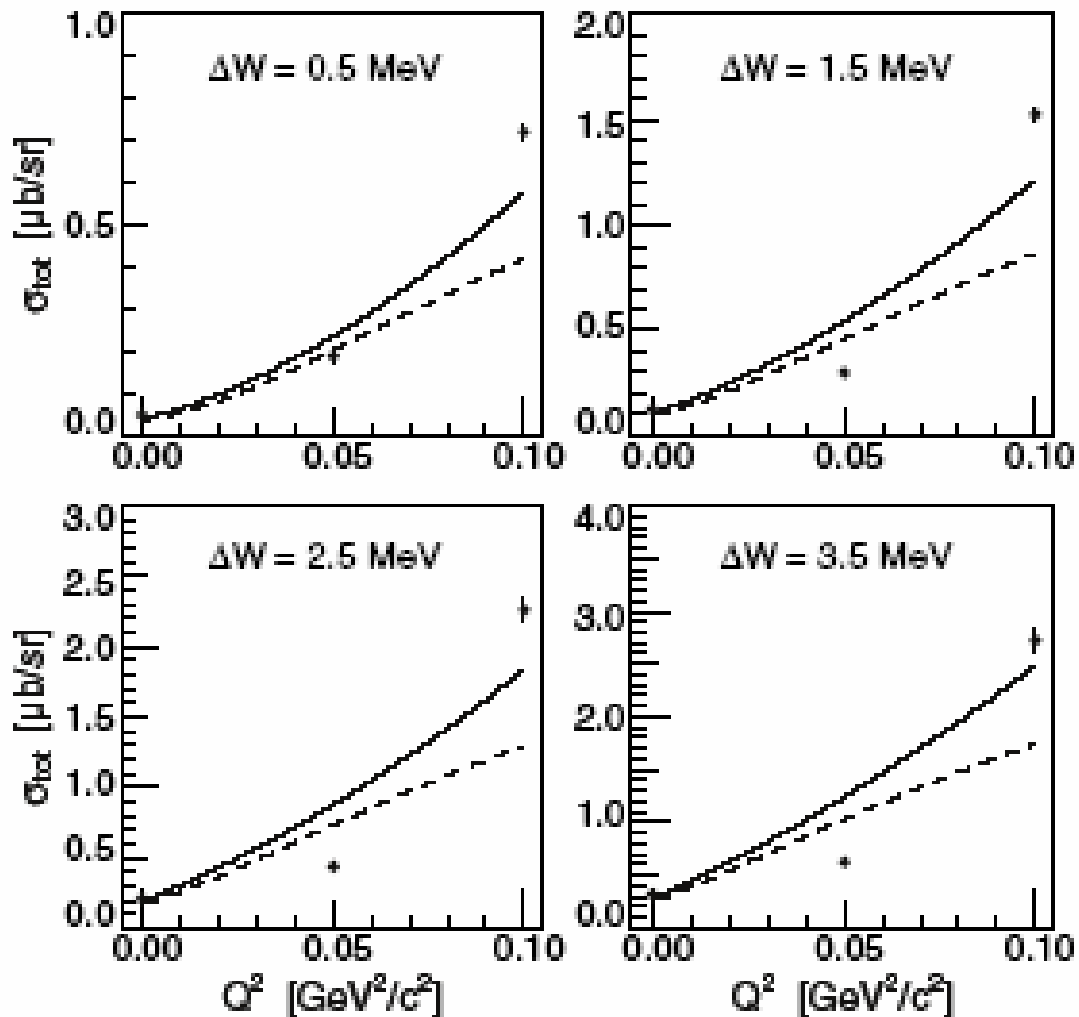


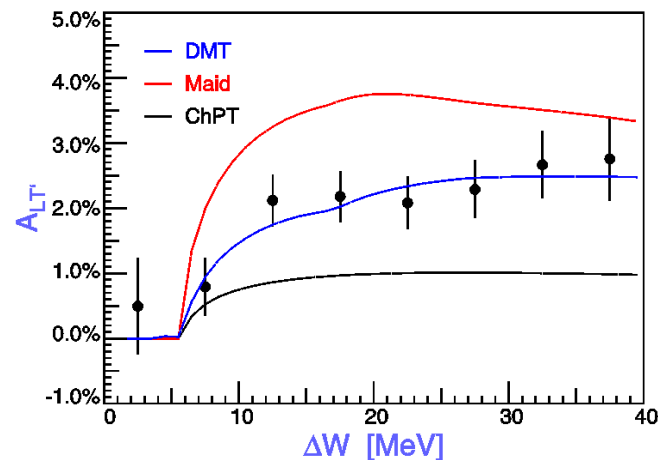
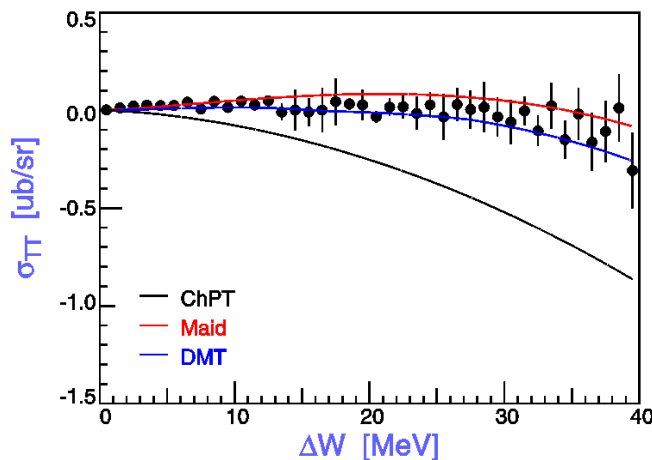
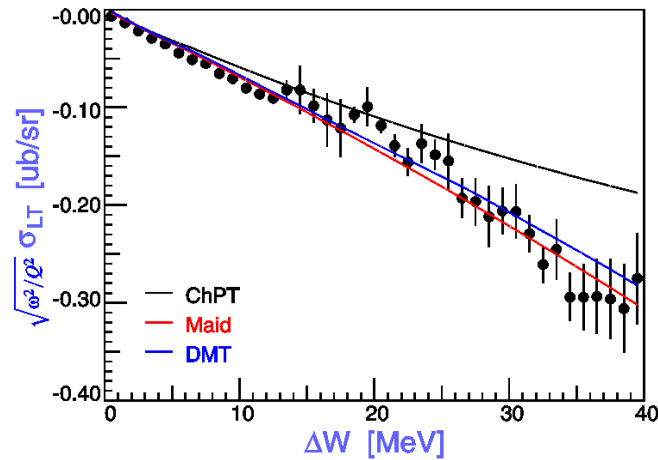
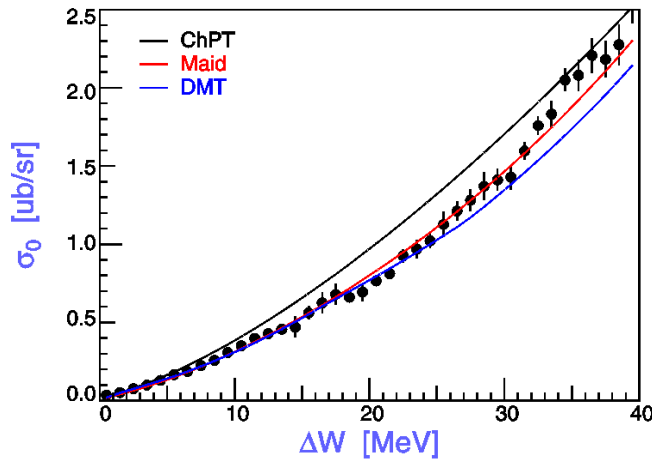
FIG. 3. The total cross section  $\sigma_{\text{tot}}$  versus  $Q^2$ , at a value of  $\epsilon = 0.8$ . The solid (dashed) line is the prediction of ChPT (MAID), data points at  $Q^2 = 0$  and  $0.1 \text{ GeV}^2/c^2$  from [6,11].

# $p(\vec{e}, e' p)\pi^0$ Electroproduction near Threshold

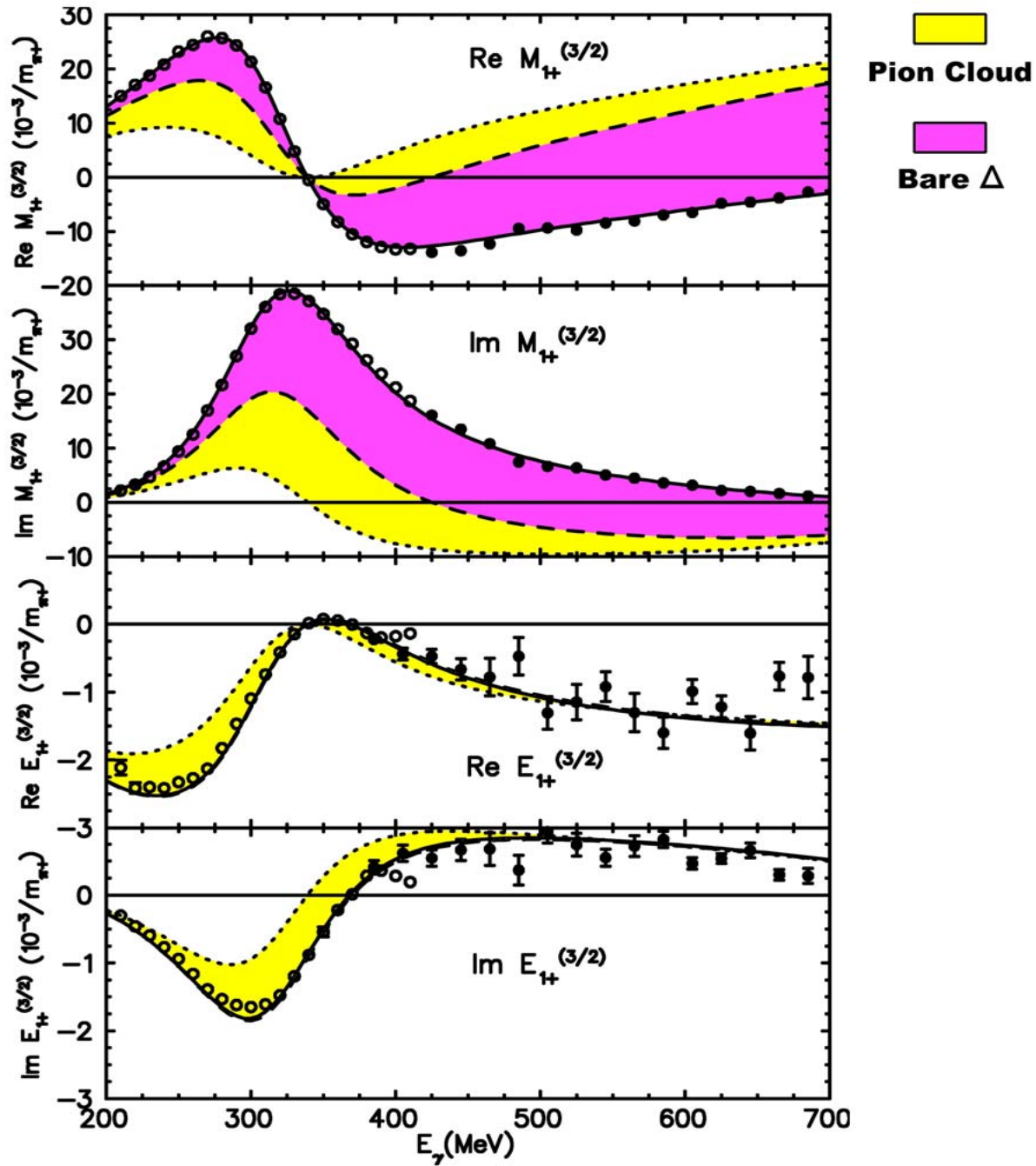
$E_0=854.5$  MeV,  $Q^2=0.05$  GeV<sup>2</sup>/c<sup>2</sup>,  $\varepsilon=0.03$ ,  $\theta=90^\circ$ ,  $\phi=90^\circ$

◆ exp. data: M. Weis, Mainz 2003

$$\frac{d\sigma_v}{d\Omega} = \frac{d\sigma_T}{d\Omega} + \varepsilon \frac{d\sigma_L}{d\Omega} + \sqrt{2\varepsilon(1+\varepsilon)} \frac{d\sigma_{LT}}{d\Omega} \cos\phi + \varepsilon \frac{d\sigma_{TT}}{d\Omega} \cos 2\phi + h\sqrt{2\varepsilon(1-\varepsilon)} \frac{d\sigma_{LT'}}{d\Omega} \sin\phi$$



$$A_{LT'} = \frac{\sqrt{2\varepsilon(1-\varepsilon)} \sigma_{LT'}}{\sigma_T + \varepsilon \sigma_L - \varepsilon \sigma_{TT}}$$



|       | $A_{1/2}$<br>( $10^{-3}GeV^{-1/2}$ ) | $A_{3/2}$      | $Q_{N! \Delta}$<br>( $fm^2$ ) | $\mu_{N! \Delta}$ |
|-------|--------------------------------------|----------------|-------------------------------|-------------------|
| PDG   | -135                                 | -255           | -0.072                        | 3.512             |
| LEGS  | -135                                 | -267           | -0.108                        | 3.642             |
| MAINZ | -131                                 | -251           | -0.0846                       | 3.46              |
| DMT   | -134<br>(-80)                        | -256<br>(-136) | -0.081<br>(0.009)             | 3.516<br>(1.922)  |
| SL    | -121<br>(-90)                        | -226<br>(-155) | -0.051<br>(0.001)             | 3.132<br>(2.188)  |

Comparison of our predictions for the helicity amplitudes,  $Q_{N! \Delta}$ , and  $\mu_{N! \Delta}$  with experiments and Sato-Lee's prediction. The numbers within the parenthesis in red correspond to the bare values.



$$\bar{A}_\alpha^\Delta(Q^2) = X_\alpha^\Delta(Q^2) \bar{A}_\alpha^\Delta(0) \frac{k}{k_w} F(Q^2), \quad \alpha=M, E, S$$

$$F(Q^2) = (1 + \beta Q^2) e^{-\gamma Q^2} G_D(Q^2), \quad G_D(Q^2) = 1 / (1 + Q^2 / 0.71)^2.$$

$\beta$  and  $\gamma$  were determined by setting  $X_M^\Delta(Q^2) \equiv 1$ ,

and fitting  $\bar{A}_\alpha^\Delta(Q^2)$  to the data for  $G_M^*$ .

$\bar{A}_M^\Delta(0)$  and  $\bar{A}_E^\Delta(0)$  were determined by fitting to the multipoles.

fitting to Jlab  $d\sigma / d\Omega$  data of  $p(e, e' p)\pi^0$  (751+867 pts)

$\Rightarrow$

$$X_E^\Delta(\text{DMT}) = 1 + Q^4 / 2.4, \quad X_S^\Delta(\text{DMT}) = 1 - 10Q^2.$$

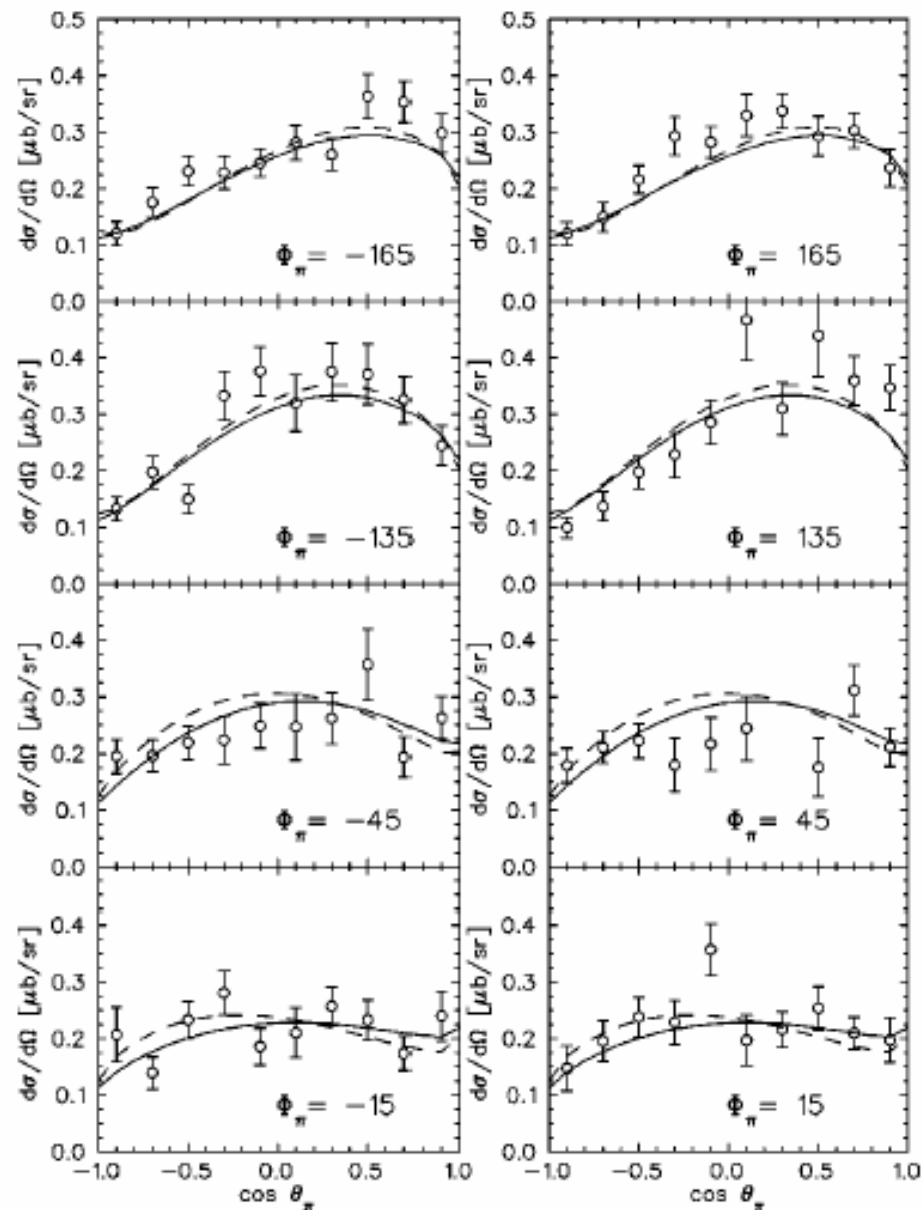
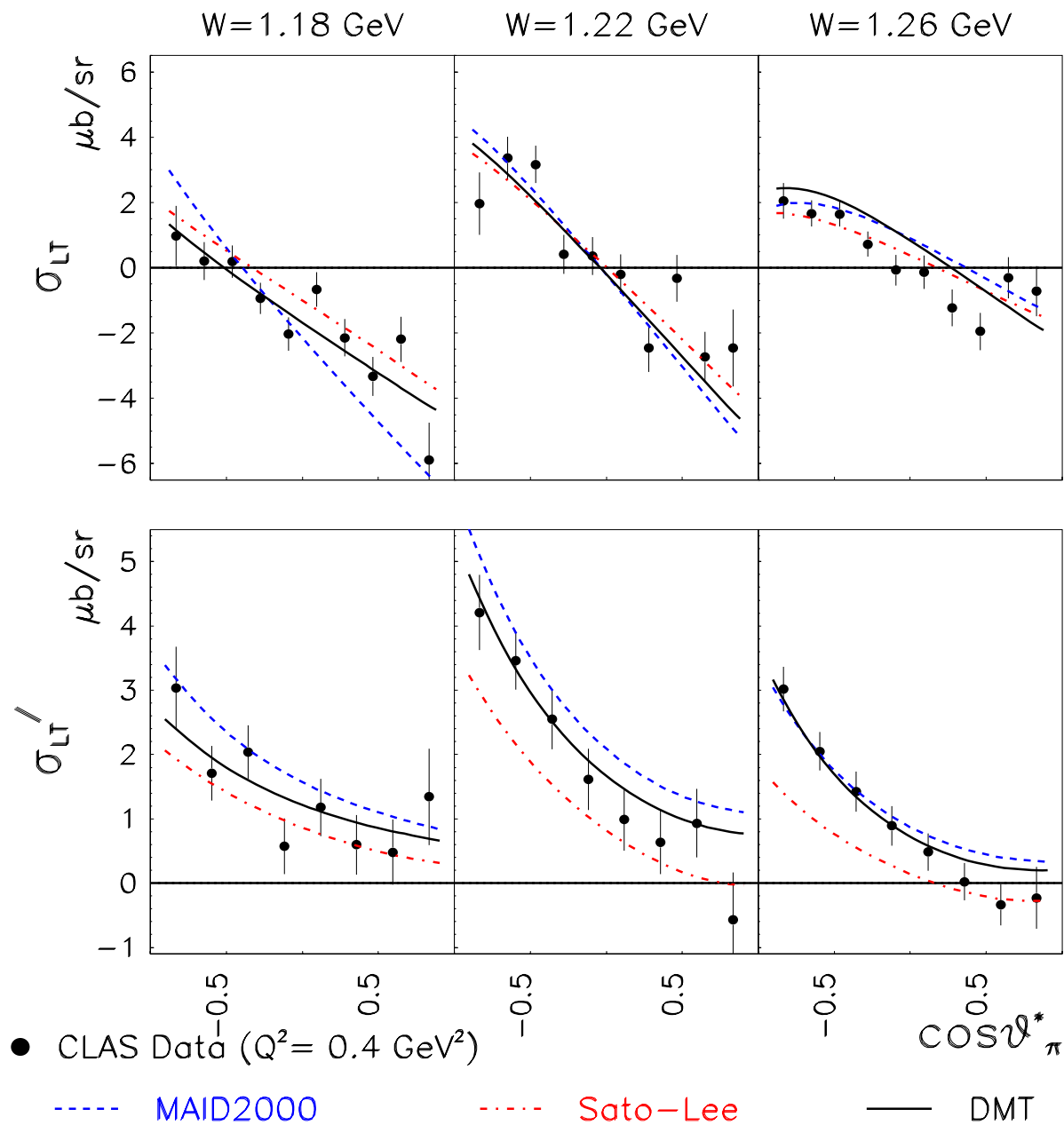
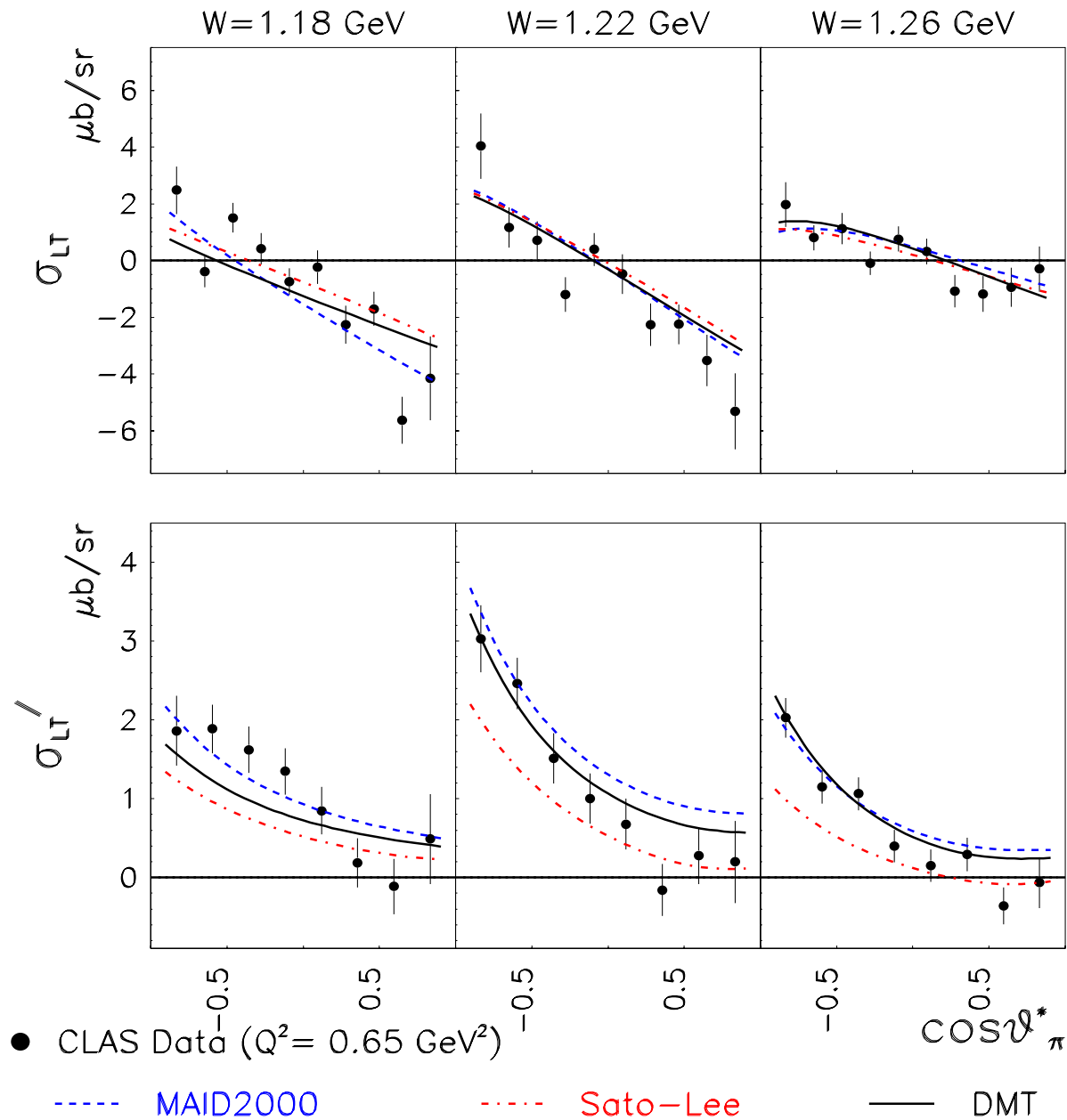


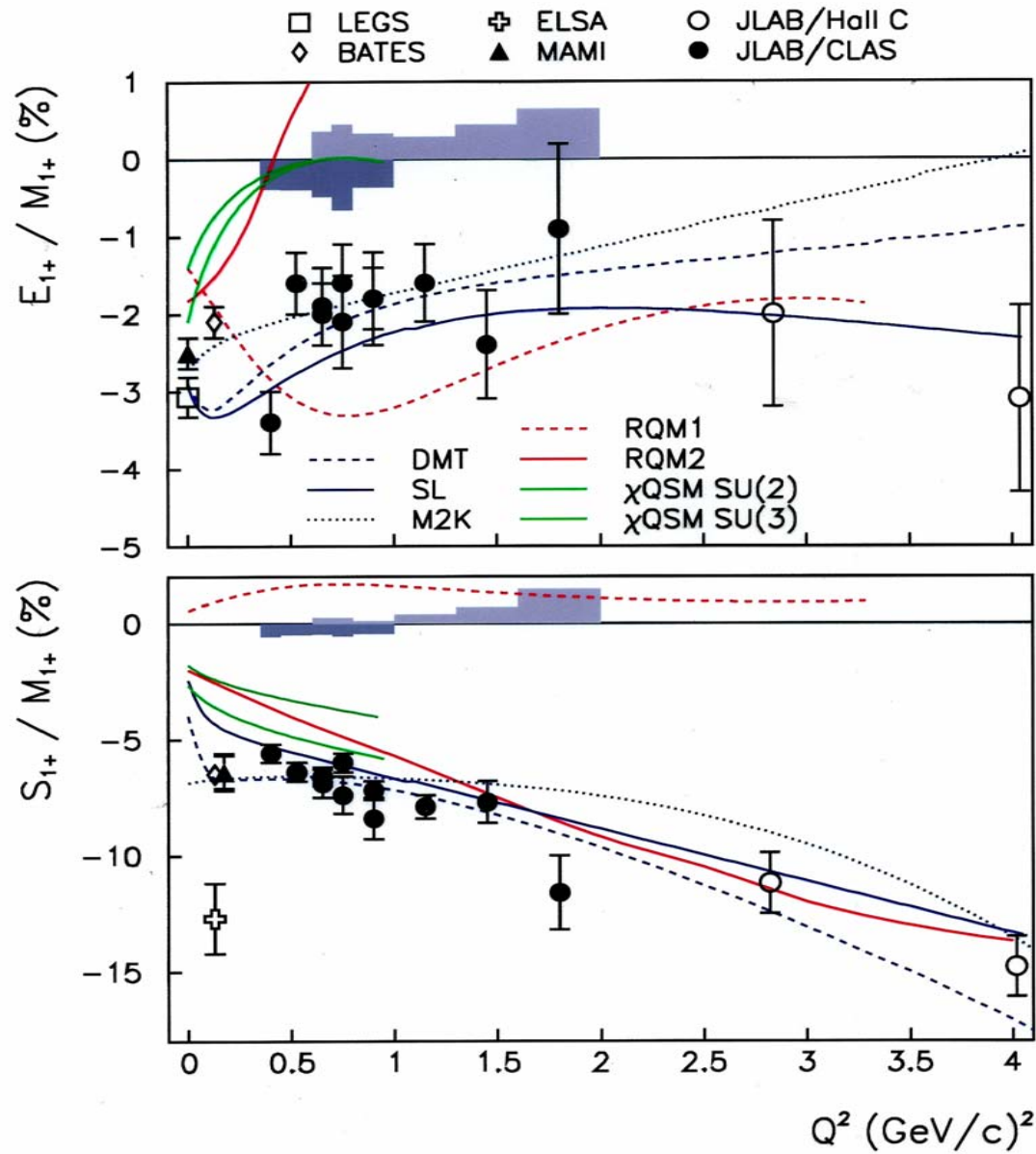
FIG. 1. The virtual photons differential cross sections at  $Q^2 = 4.03 \text{ (GeV}/c)^2$  and  $W = 1232 \text{ MeV}$ . The full and dashed curves are the results from the MAID and DM analysis, respectively. Data are from Ref. [1].

# L-T Interference Structure Functions



# L-T Interference Structure Functions





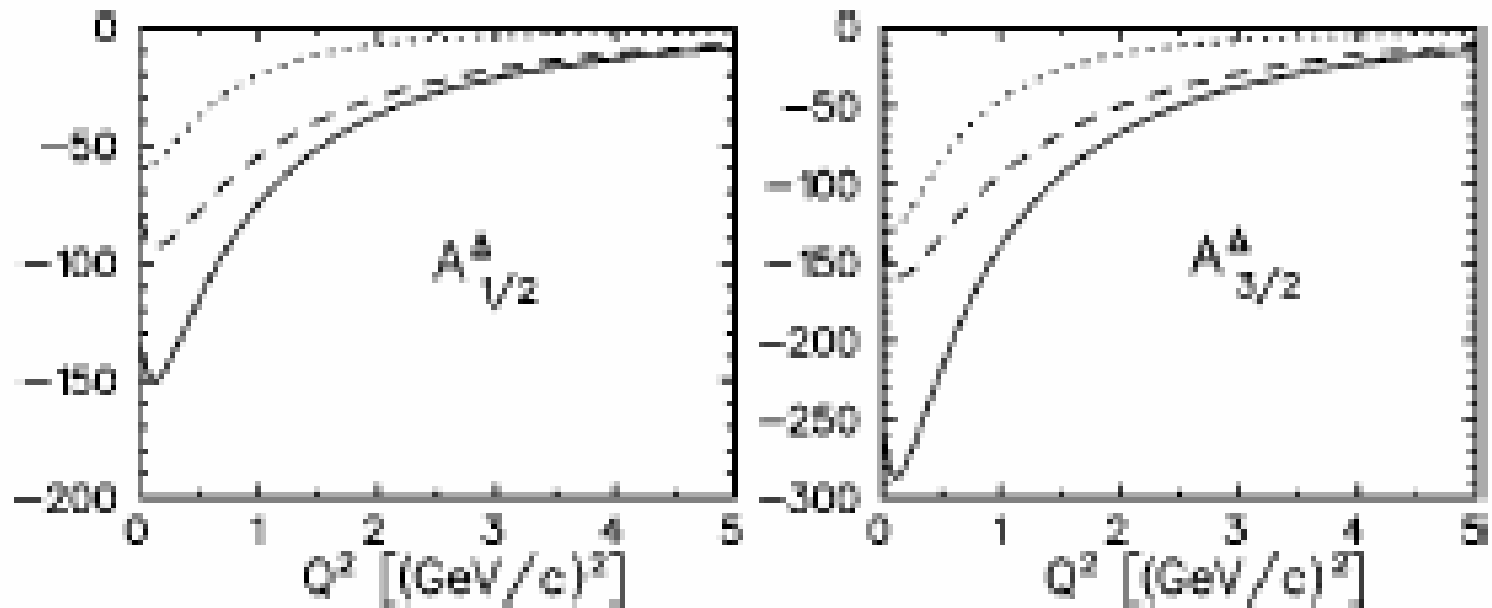


FIG. 4. The  $Q^2$  dependence of the bare (dashed curves) and dressed (solid curves) helicity amplitudes  $A_{1/2}$  and  $A_{3/2}$  (in units of  $10^{-3} \text{ GeV}^{-1/2}$ ) extracted with DM. The dotted curves are the pion cloud contributions.

$A_{1/2} \neq A_{3/2}$ , hadron helicity conservation not yet observed

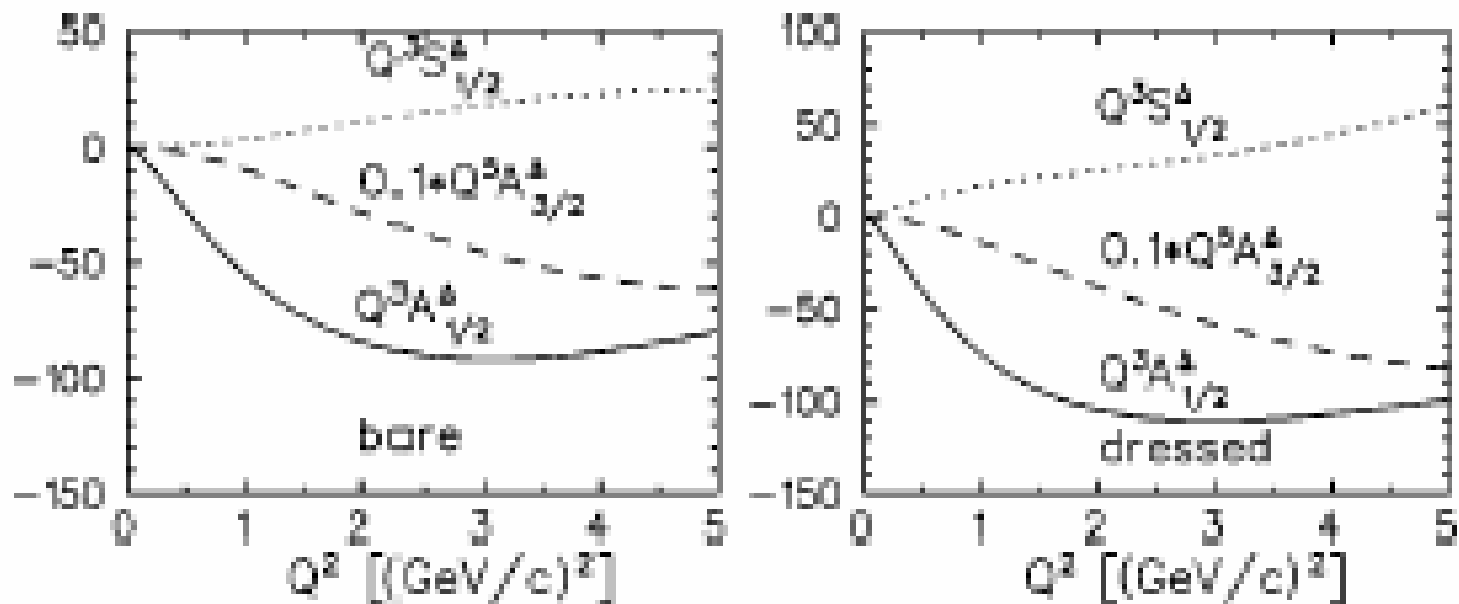


FIG. 5. The  $Q^2$  dependence of the  $Q^3 A_{1/2}^{\Delta}$  (solid curve),  $Q^5 A_{3/2}^{\Delta}$  (dashed curve), and  $Q^3 S_{1/2}^{\Delta}$  (dotted curve) amplitudes (in units of  $10^{-3} \text{ GeV}^{m/2}$ ) obtained with DM.

bare  $S_{1/2}^{\Delta}$  and  $A_{1/2}^{\Delta}$  start exhibiting pQCD scaling behavior

# Extension to higher energies

---

➤ coupled  $\pi$ ,  $\eta$ ,  $2\pi$  channels

$$t_{ij}(E) = v_{ij} + \sum_k v_{ik} g_k(E) t_{kj}(E),$$

$(i, j, k = \pi, \eta)$

➤ Include resonances R's with couplings to  $\pi$ ,  $\eta$ ,  $2\pi$  channels

$$v_{ij}(E) = v_{ij}^B(E) + v_{ij}^R(E)$$



Non-resonant background  $v_{ij}^B$  :

$v_{\pi\pi}^B$  as given before,

$$v_{\pi\eta}^B = v_{\eta\pi}^B = v_{\eta\eta}^B = 0.$$

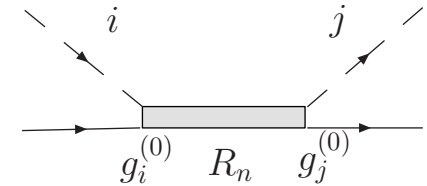
$$L_I = ig_{\pi NR}^{(0)} \overline{R} \boldsymbol{\tau} \cdot \boldsymbol{\pi} N + ig_{\eta NR}^{(0)} \overline{R} \eta N + \text{h.c.}$$

Resonance contribution  $v_{ij}^R$  :

$$v_{ij}^R = \sum_{n=1}^N v_{ij}^{R_n}(q', q; E),$$

for N overlapping resonances.

$$v_{ij}^{R_n} = \frac{f(\Lambda_i^{(n)}, q'; E) g_i^{(0)} g_j^{(0)} f(\Lambda_j^{(n)}, q; E)}{E - M_{R_n}^{(0)} + i \frac{1}{2} \Gamma_{2\pi}^{(n)}(E)},$$

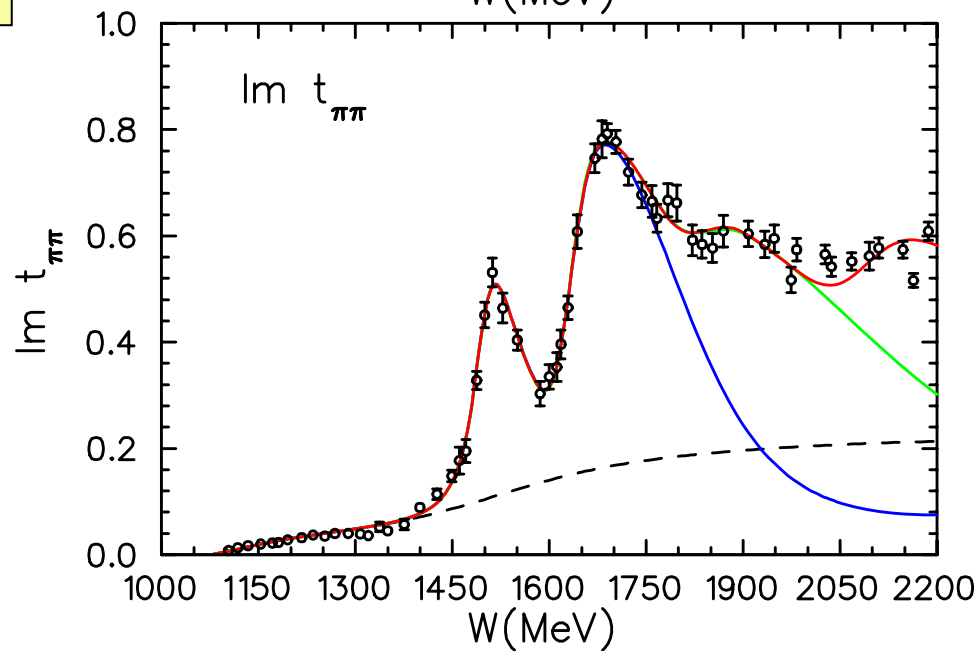
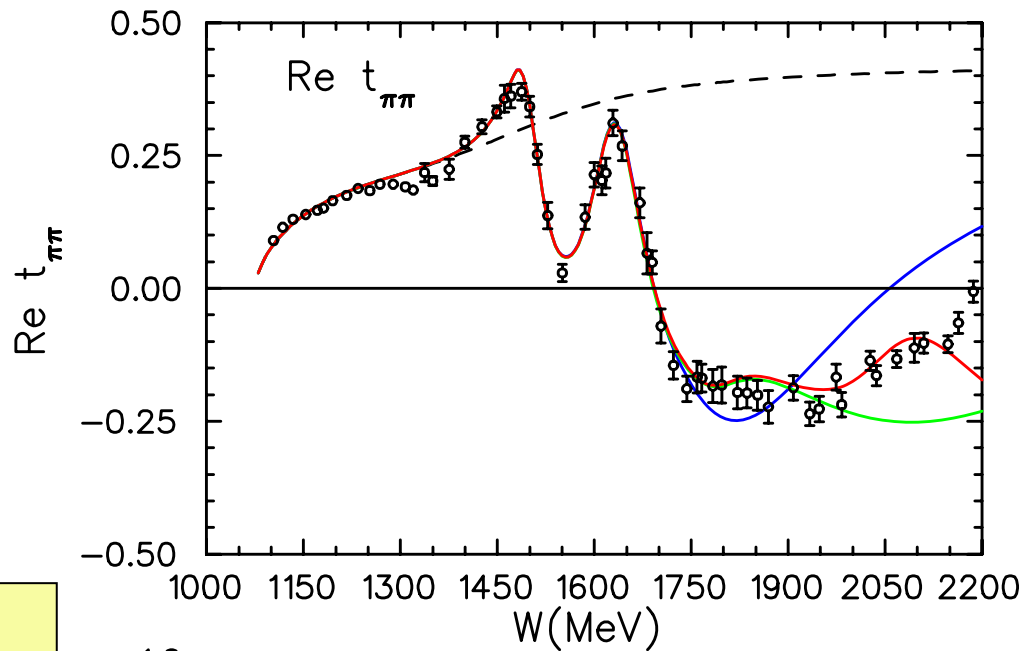


$M_{R_n}^{(0)}$  = bare mass of resonance  $R_n$ ,

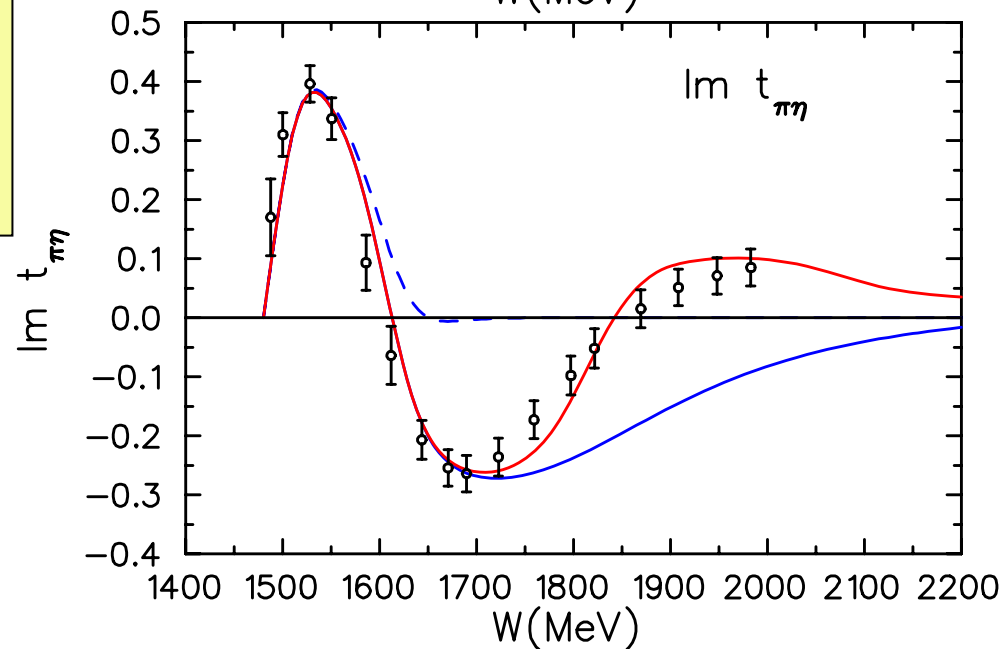
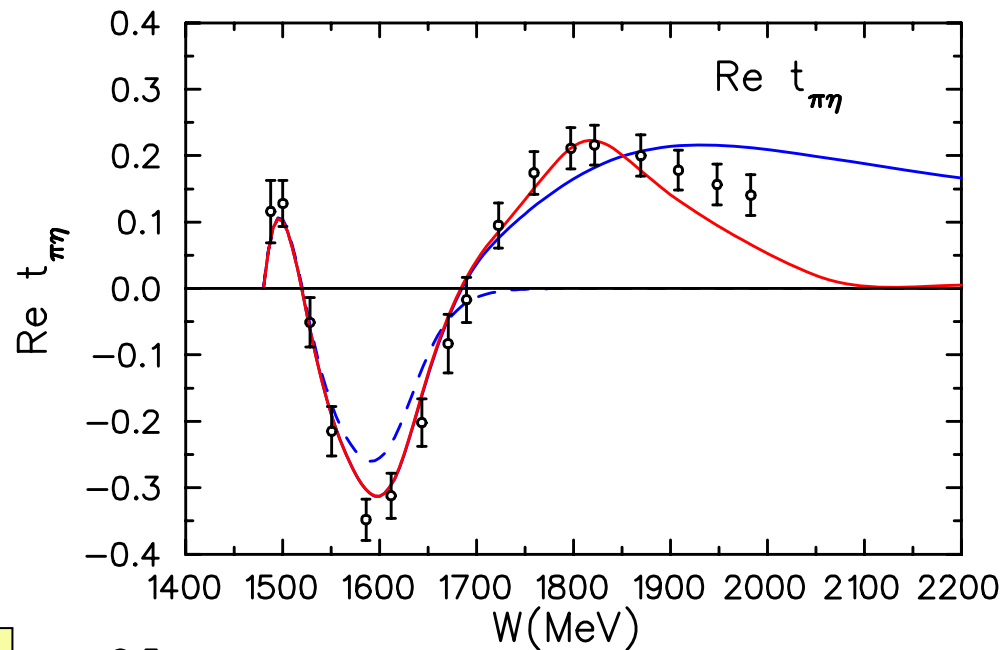
$$\Gamma_{2\pi}^{(n)} = \Gamma_{2\pi}^{0,n} \left( \frac{q_{2\pi}}{q_{0,n}} \right)^{2l+4} \left( \frac{X^2 + q_{0,n}^2}{X^2 + q_{2\pi}^2} \right)^{l+2}$$

= effects of  $\pi\pi N$  decay channel

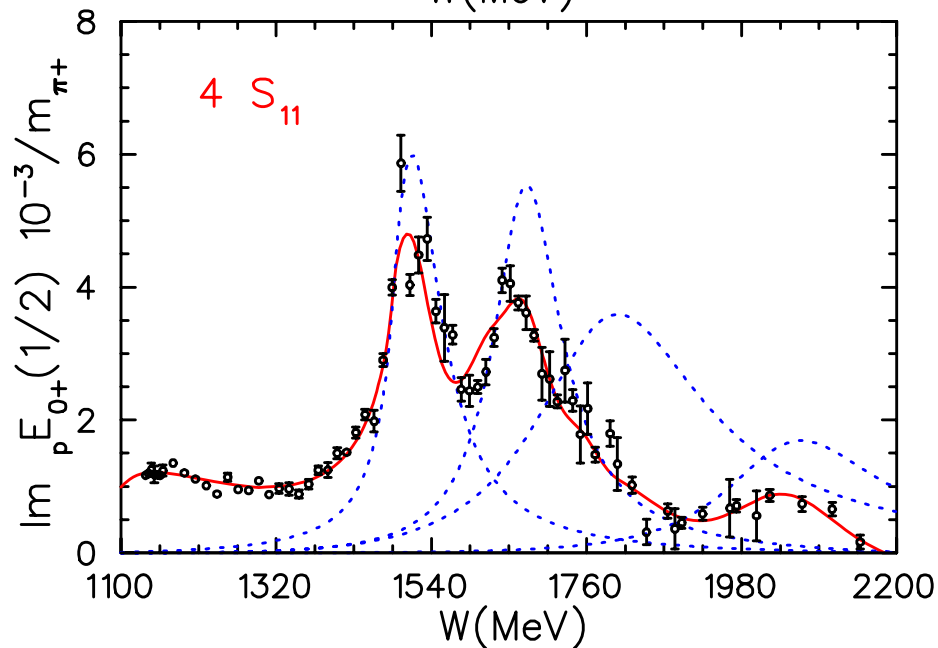
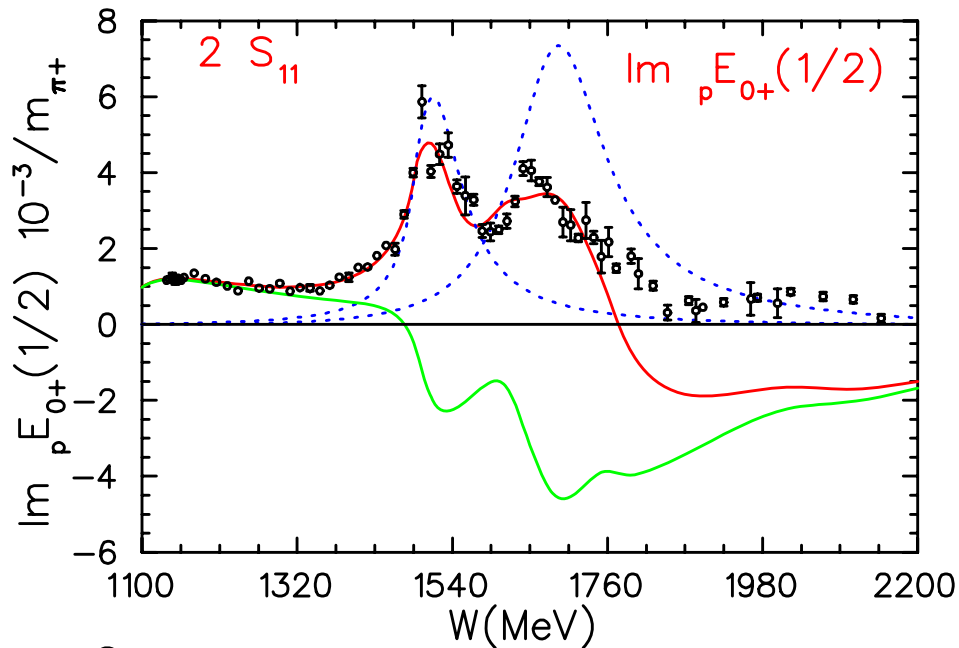
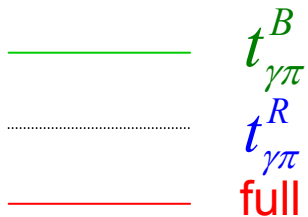
— 2R  
— 3R  
— 4R



----- 1R  
——— 2R  
——— 3R

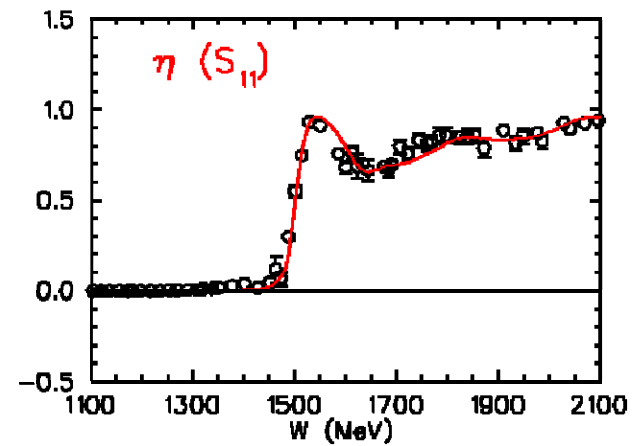
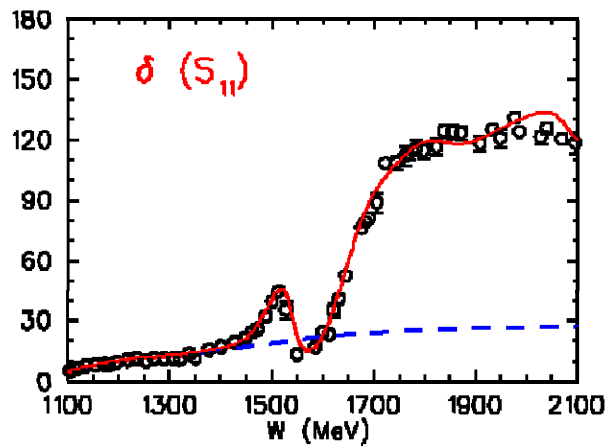
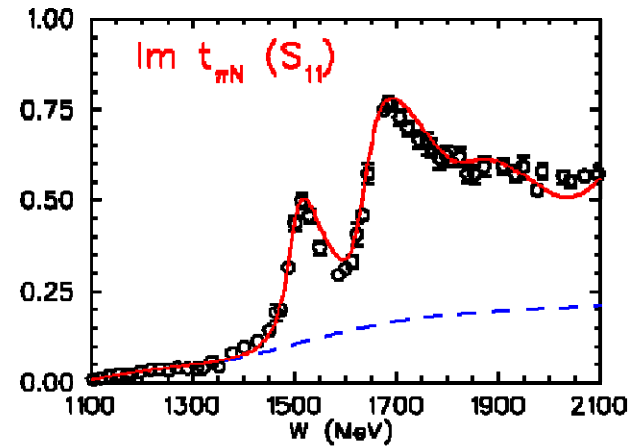
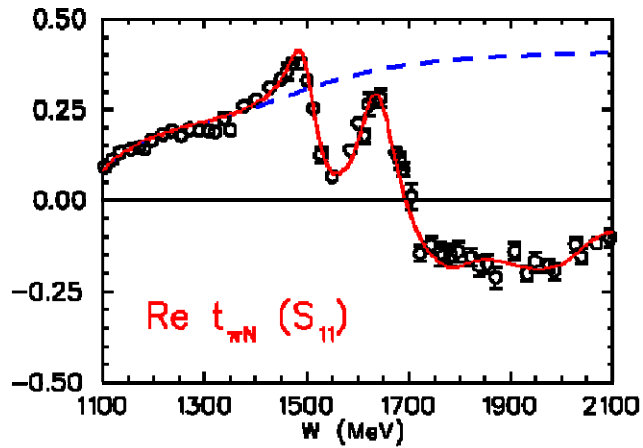


No evidence for the  
4th  $S_{11}$  resonance in  
 $\pi N \rightarrow \eta N$

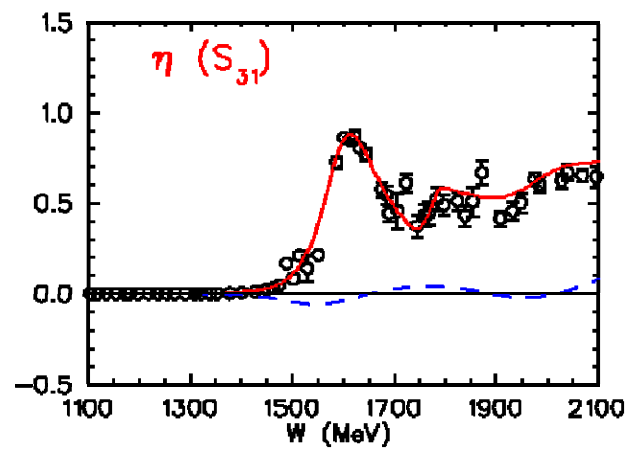
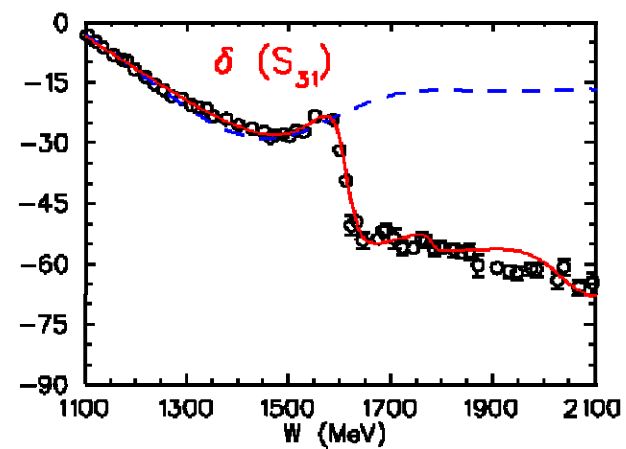
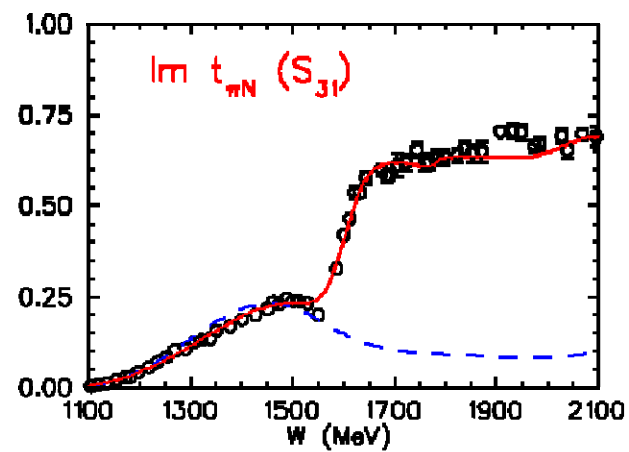
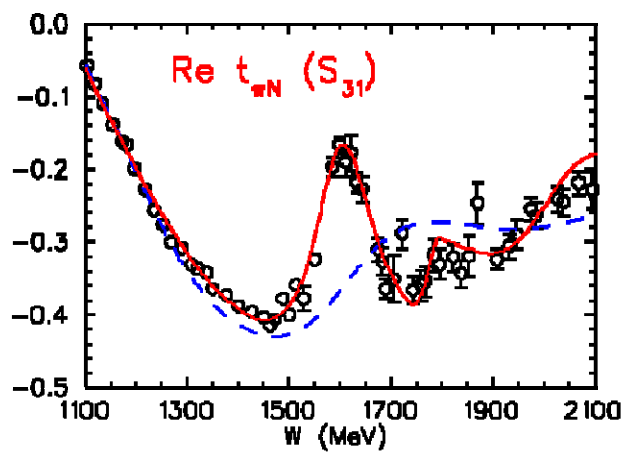


**Need 4  $S_{11}$   
 Resonances**

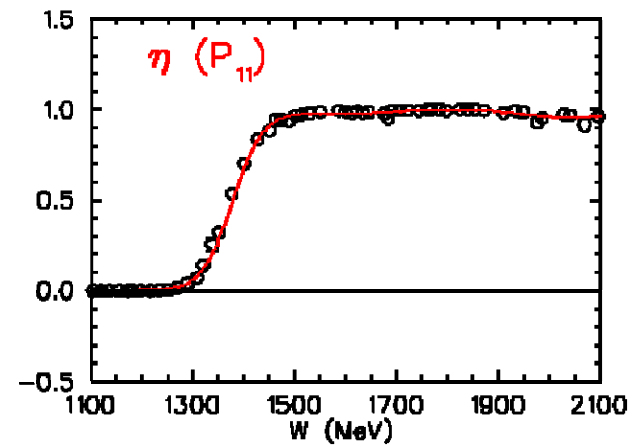
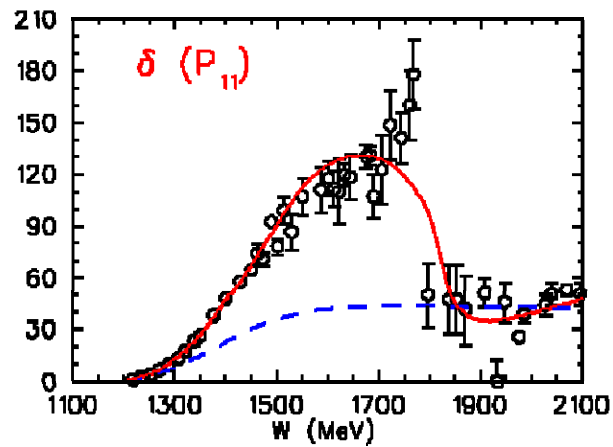
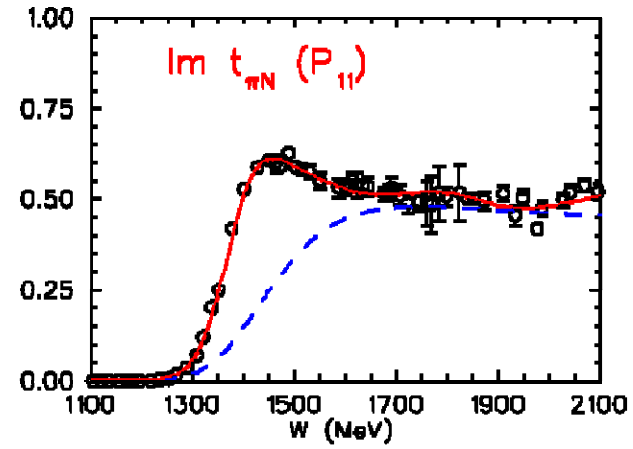
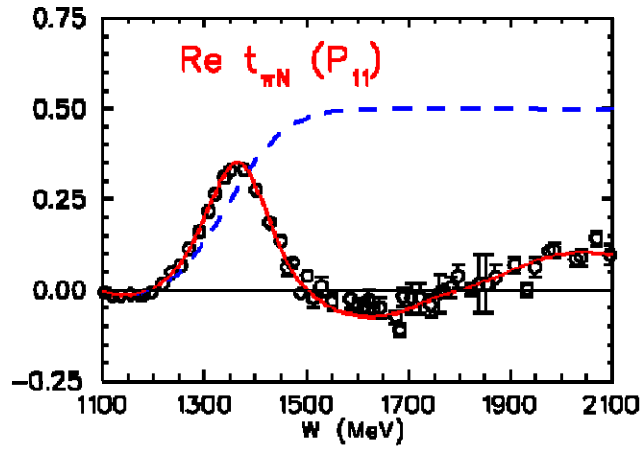
(3,4), red- PDG, blue- DMT



(3,3)

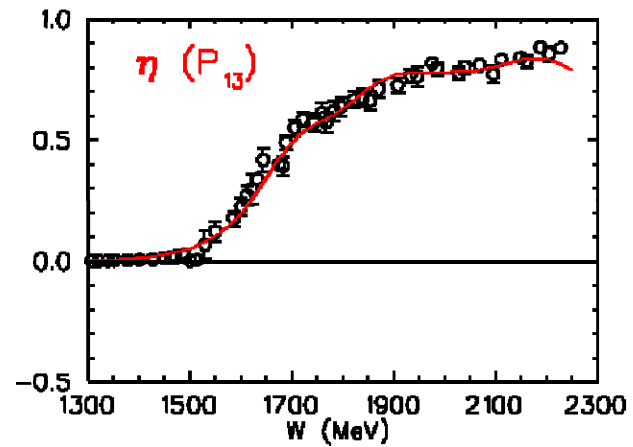
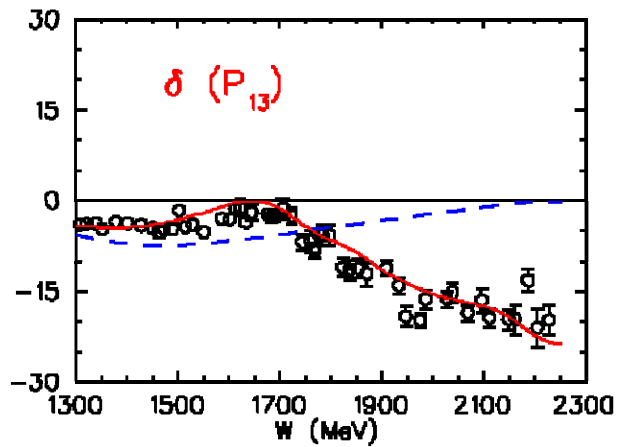
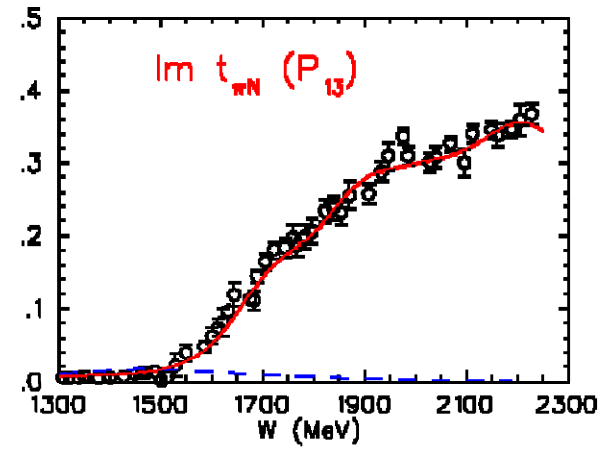
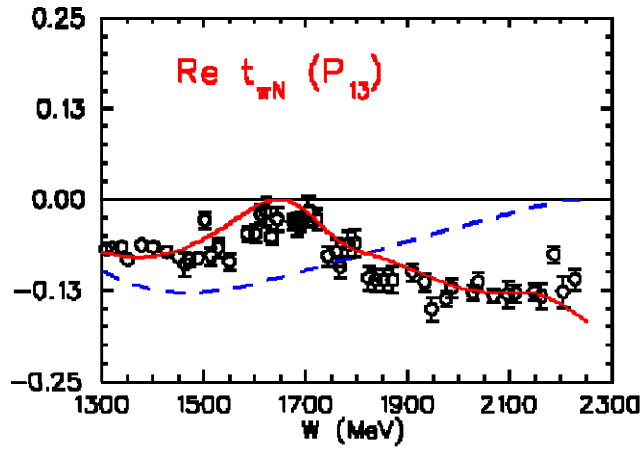


(3,3)

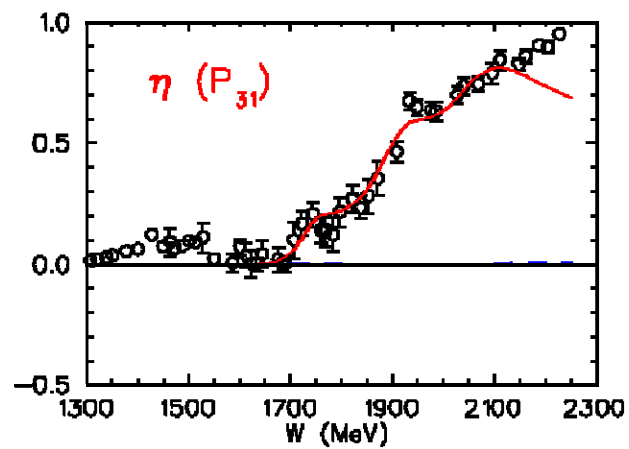
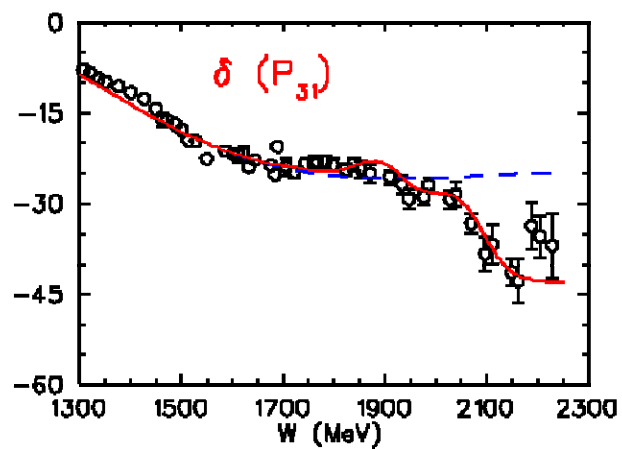
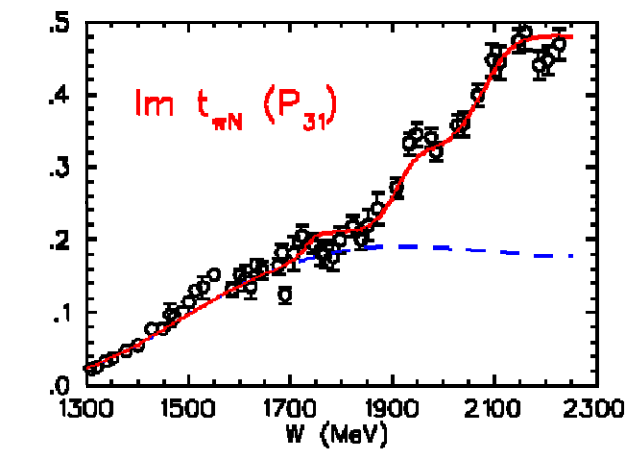
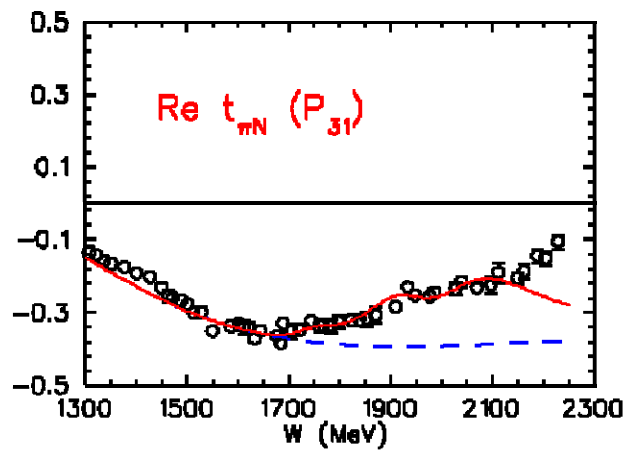




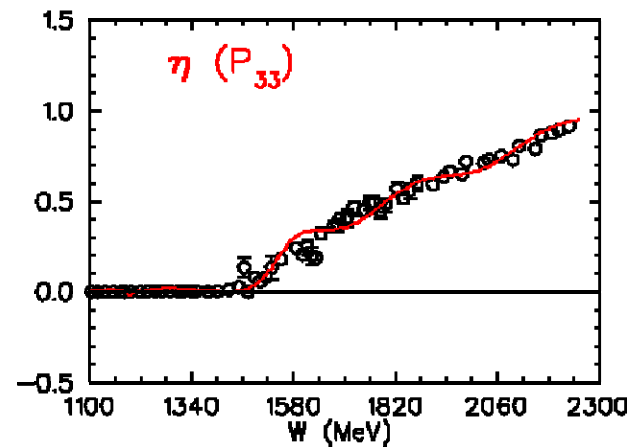
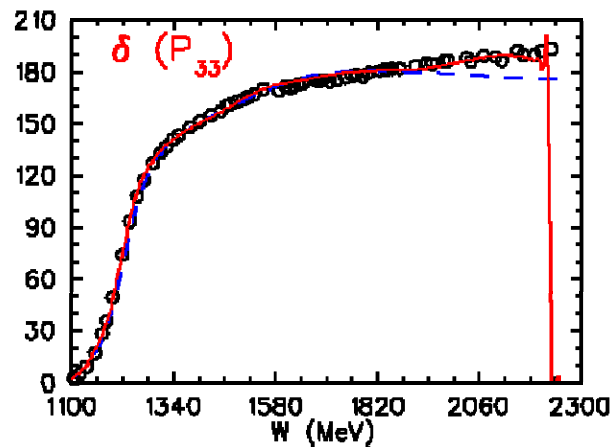
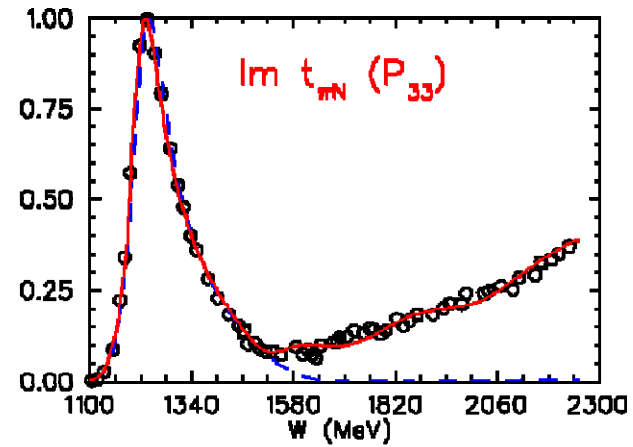
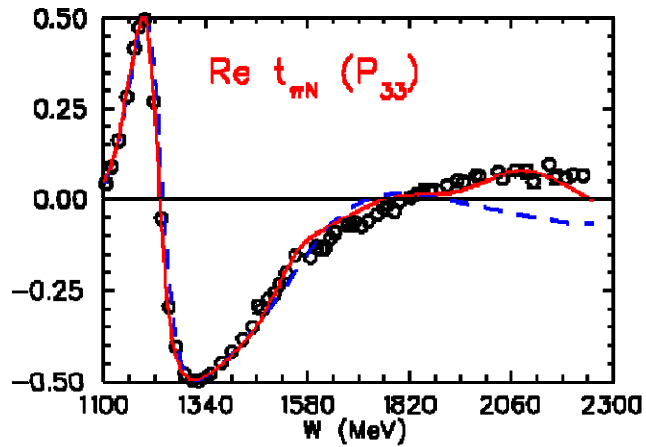
(2,2)



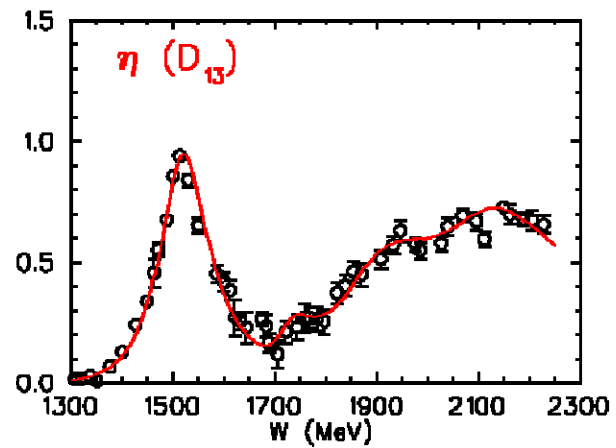
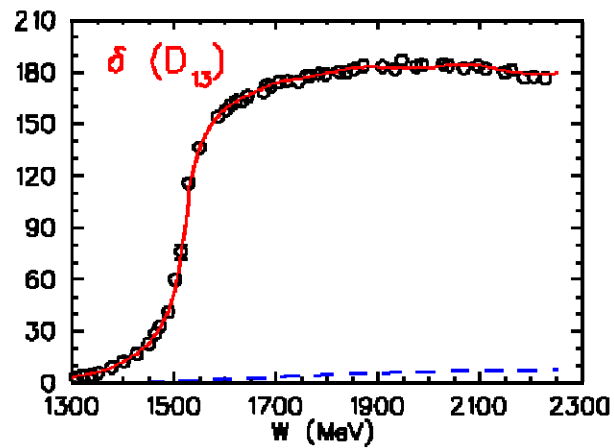
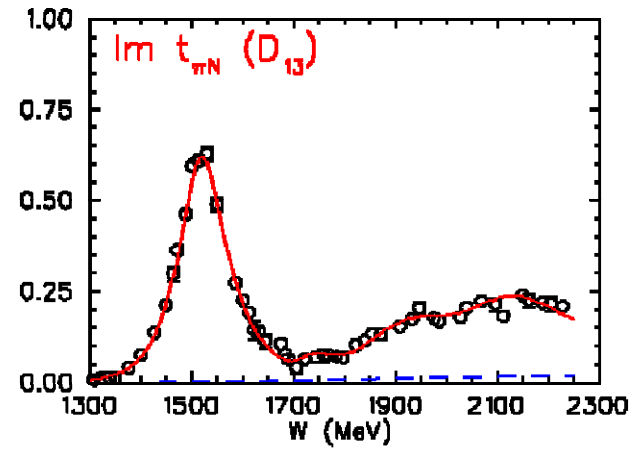
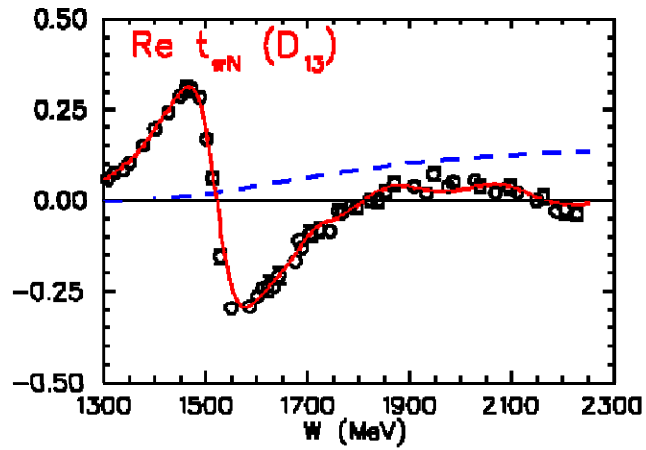
(2,3)



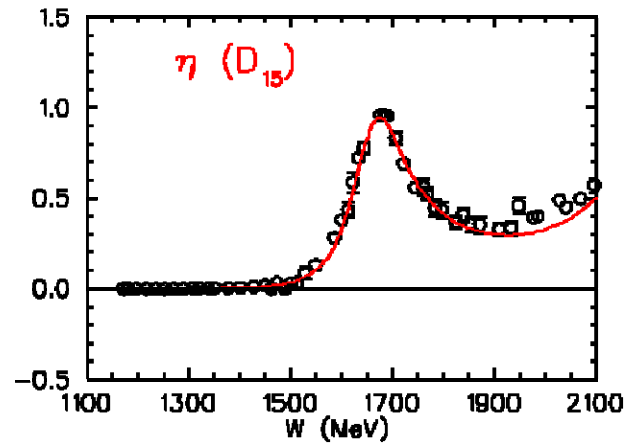
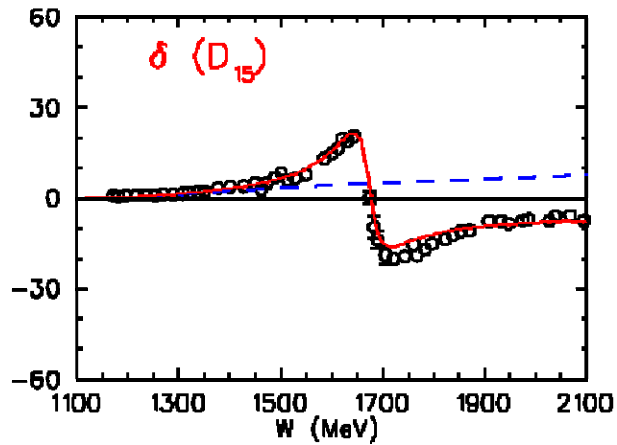
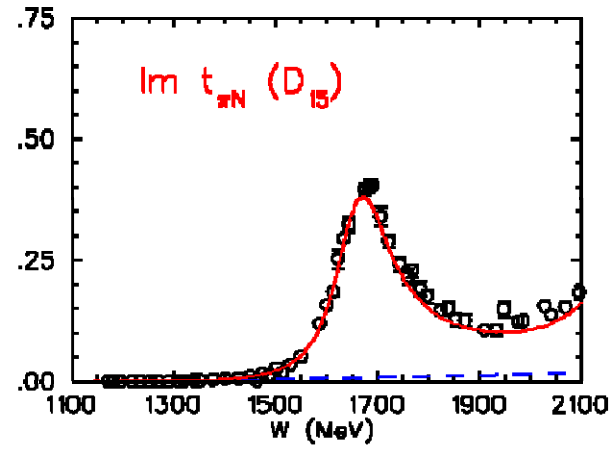
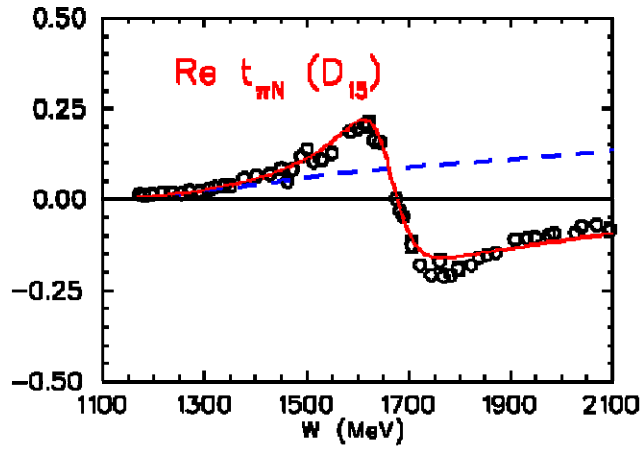
(3,3)



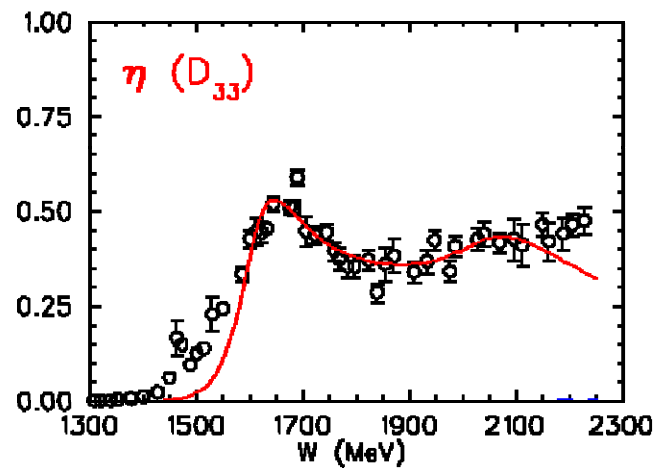
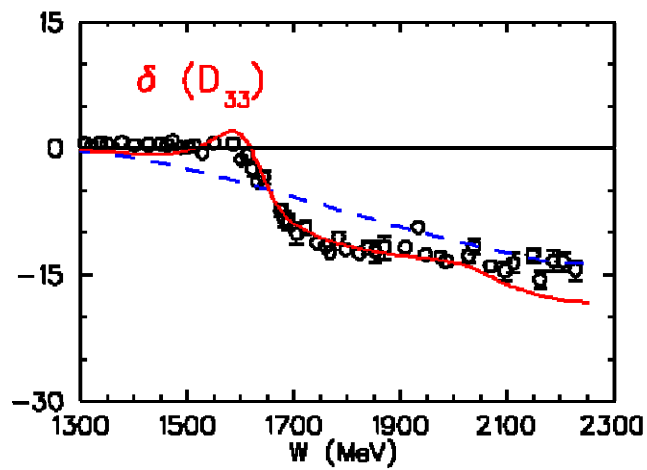
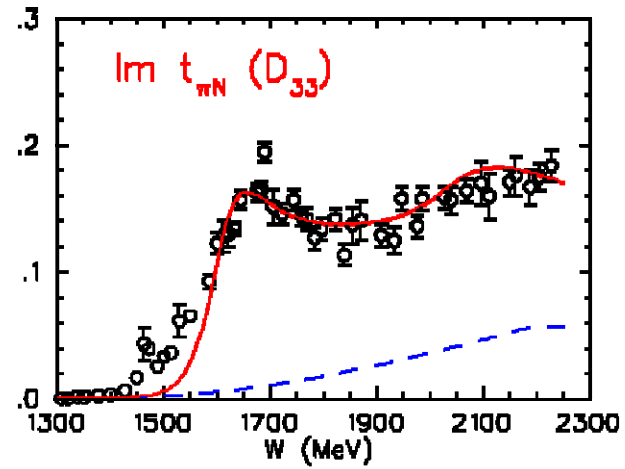
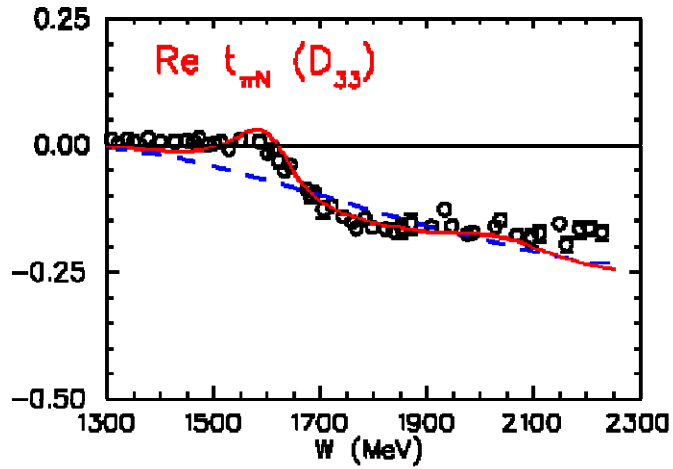
(3,3)



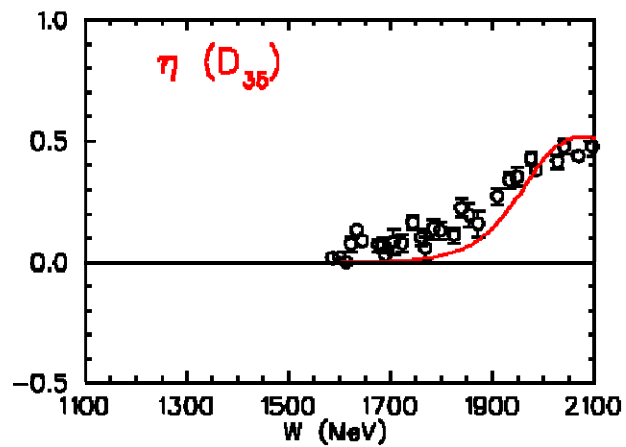
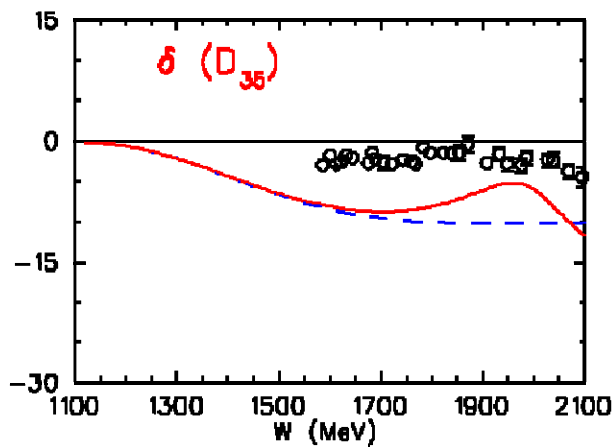
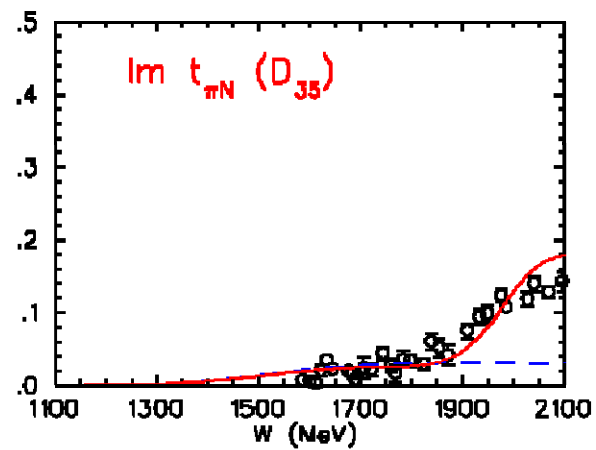
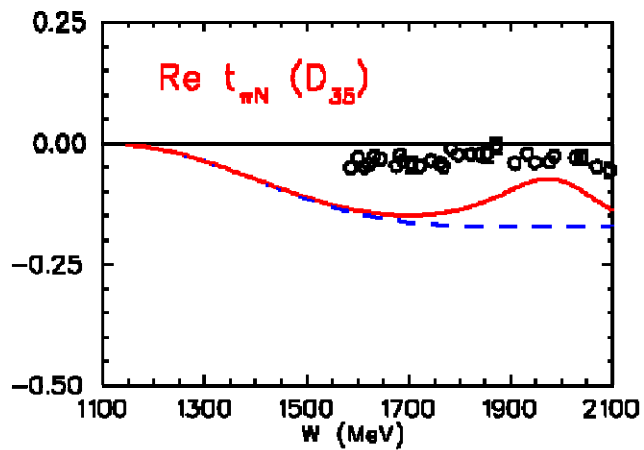
(2,2)



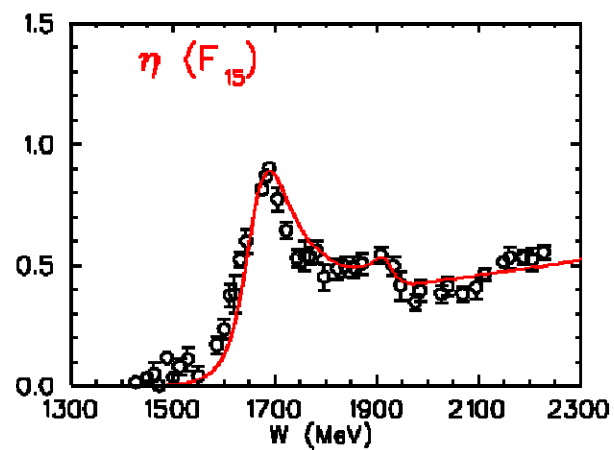
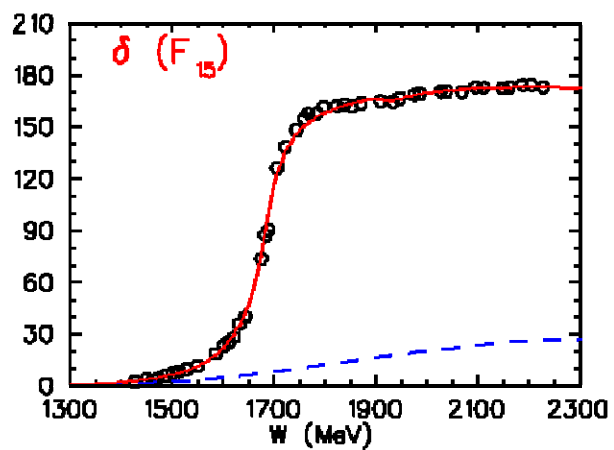
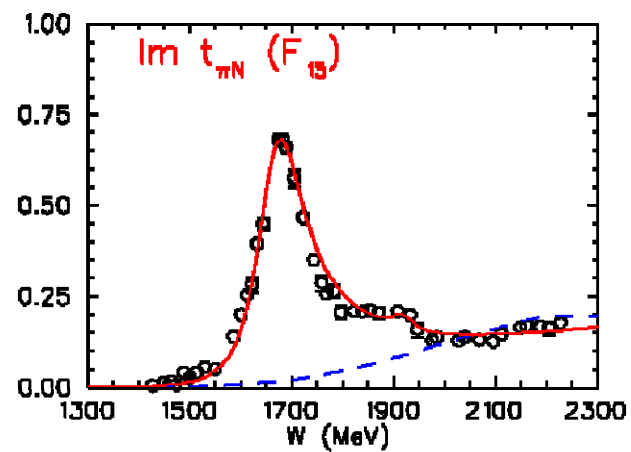
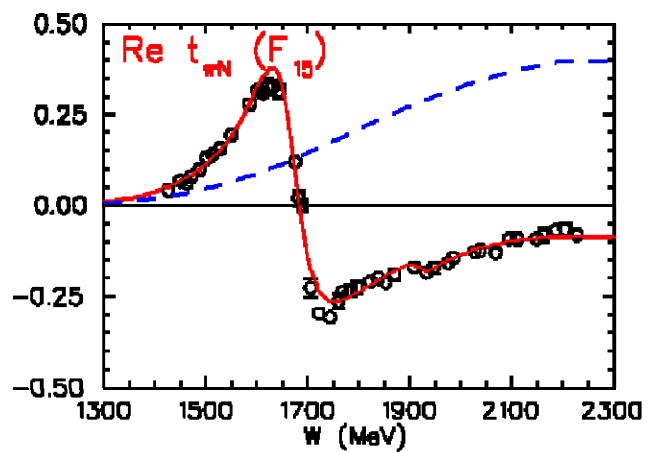
(2,2)



(2,1)

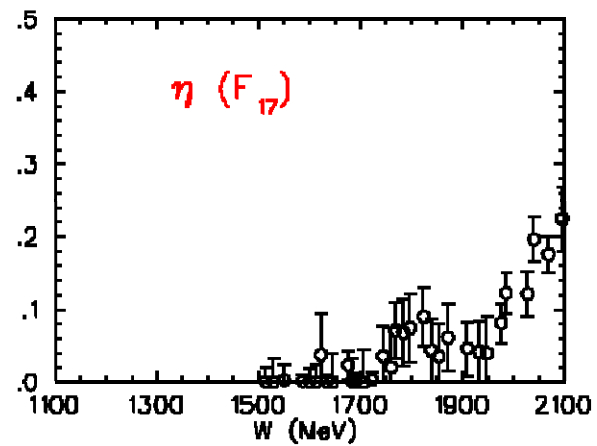
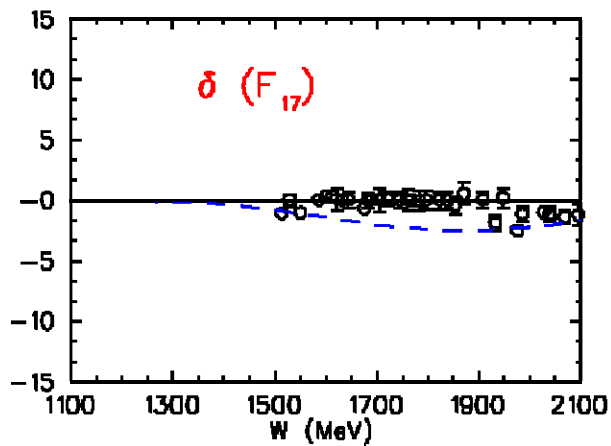
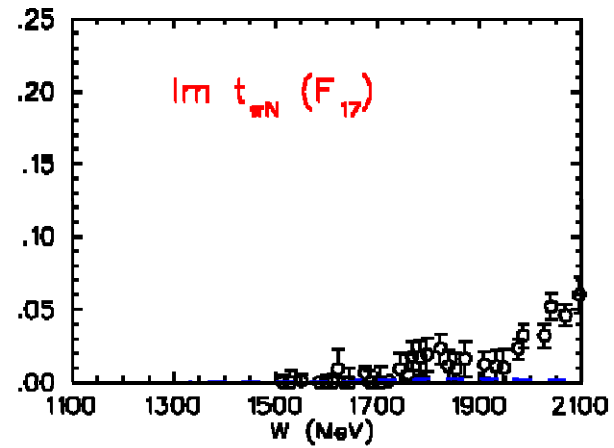
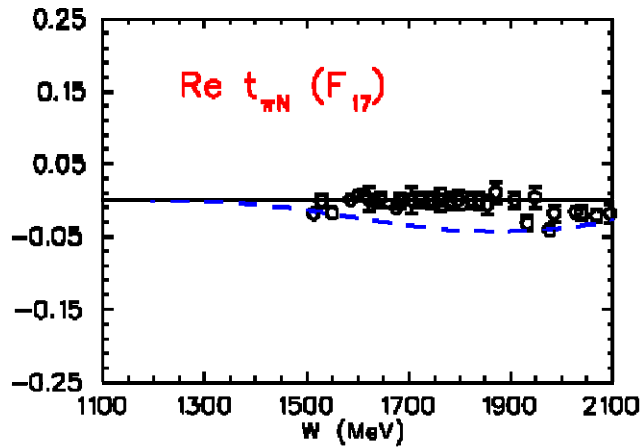


(2,2)

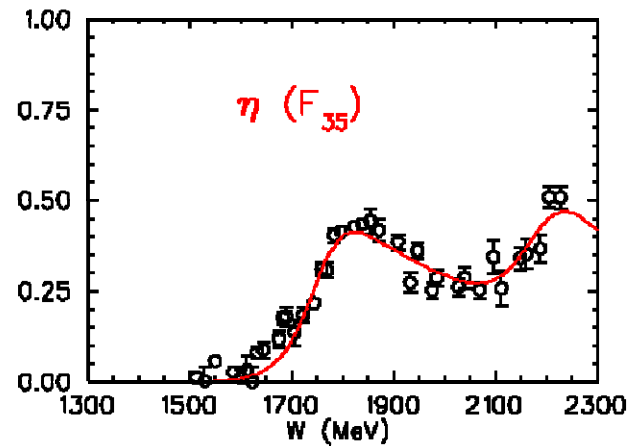
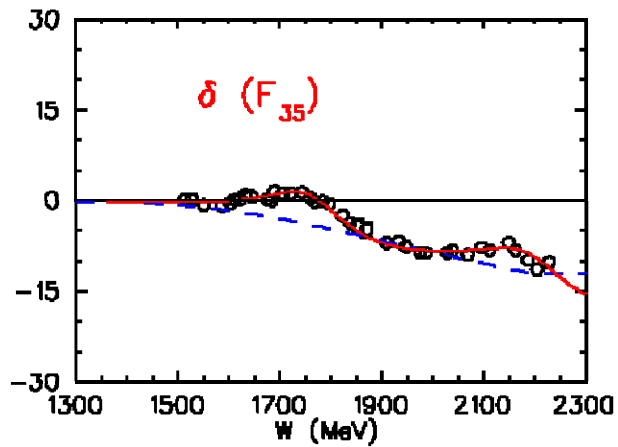
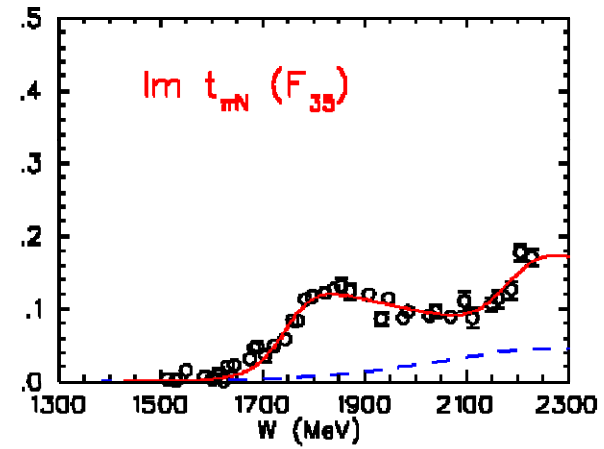
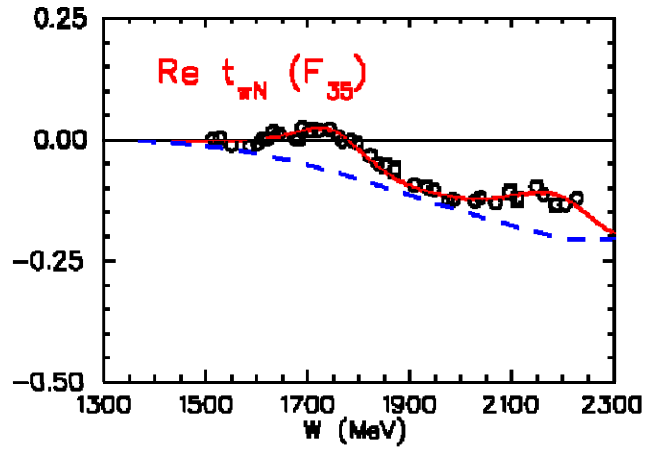




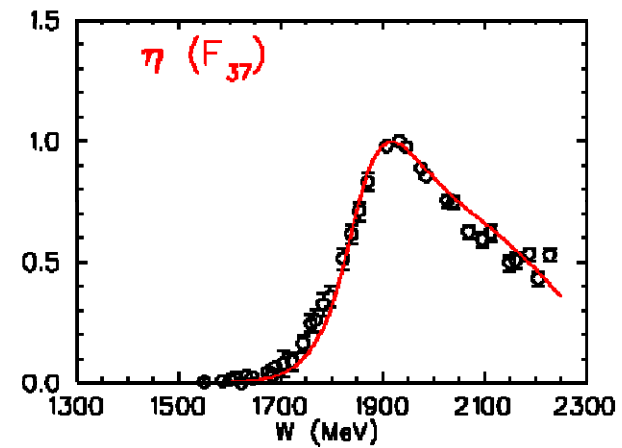
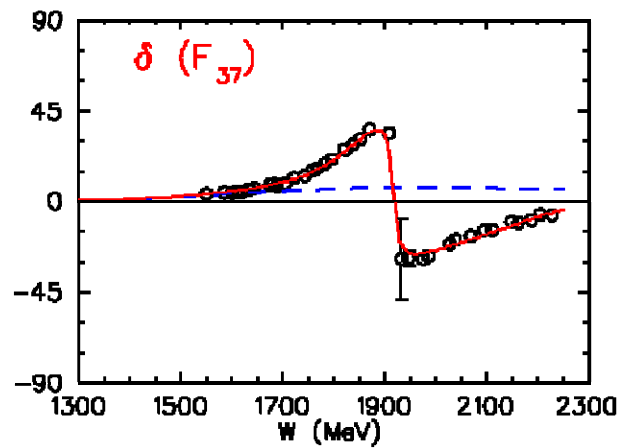
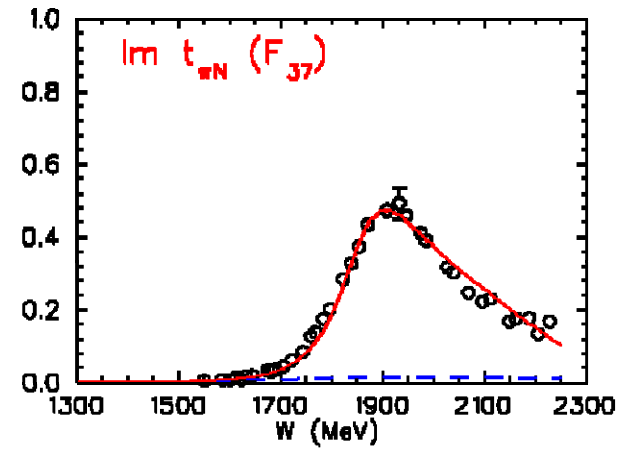
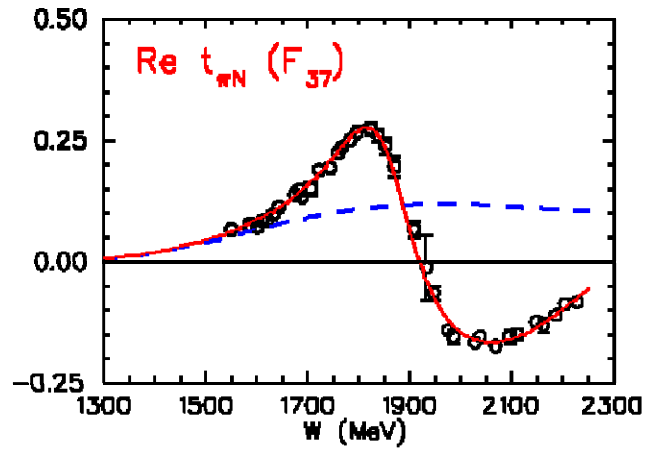
(1,0)



(2,2)



(2,1)



## Pole Positions and Residues in [ MeV ] (preliminary)

| N*                    | 1st Resonance   |   | 2nd Resonance  |  | 3rd Resonance  |  |
|-----------------------|---|---|--|--|--|--|
|                       | Wp  | $\Gamma_p$  | Wp   | $\Gamma_p$   | Wp   | $\Gamma_p$   |
| S <sub>11</sub> (3,4) | 1499<br><span style="color: red;">(1505, 1501)</span> | 67<br><span style="color: blue;">(170, 124)</span>  | 1642<br><span style="color: blue;">(1660, 1673)</span> | 97<br><span style="color: blue;">(160, 82)</span>    | 2065<br><span style="color: green;">(2150±70)</span>       | 223<br><span style="color: green;">(350±100)</span>      |
| S <sub>31</sub> (3,3) | 1598<br><span style="color: red;">(1600, 1585)</span> | 136<br><span style="color: blue;">(115, 104)</span> | 1775<br><span style="color: green;">(1870±40)</span>   | 36<br><span style="color: green;">(1850±50)</span>   | 2012<br><span style="color: green;">(2140±80)</span>       | 148<br><span style="color: green;">(200±80)</span>       |
| P <sub>11</sub> (3,3) | 1366<br><span style="color: red;">(1365, 1346)</span> | 179<br><span style="color: blue;">(210, 176)</span> | 1721<br><span style="color: blue;">(1720, 1770)</span> | 185<br><span style="color: blue;">(230, 378)</span>  | 1869<br><span style="color: green;">(2120±40, 1810)</span> | 238<br><span style="color: orange;">(240±80, 622)</span> |
| P <sub>13</sub> (2,2) | 1683<br><span style="color: red;">(1700, 1717)</span> | 239<br><span style="color: blue;">(250, 388)</span> | 1846<br><span style="color: red;">(not listed)</span>  | 180<br><span style="color: red;">(not listed)</span> |  |  |
| P <sub>31</sub> (2,3) | 1729<br><span style="color: orange;">(1714)</span>    | 70<br><span style="color: orange;">(68)</span>      | 1896<br><span style="color: blue;">(1855, 1810)</span> | 130<br><span style="color: blue;">(350, 494)</span>  | 2065   | 161  |
| P <sub>33</sub> (3,3) | 1218<br><span style="color: red;">(1210, 1211)</span> | 90<br><span style="color: blue;">(100, 100)</span>  | 1509<br><span style="color: blue;">(1600, 1675)</span> | 236<br><span style="color: blue;">(300, 386)</span>  | 2149<br><span style="color: green;">(1900, 1900±80)</span> | 400<br><span style="color: green;">(300, 300±100)</span> |

Red □ PDG04

Blue □ Arndt95

Green □ Cutkovsky80

Orange □ Vrana00

obtained with speed plot

## Pole Positions and Residues in [ MeV ] (preliminary)

| N*                    | 1st Resonance                       |                                  | 2nd Resonance                               |  | 3rd Resonance                     |                                |
|-----------------------|-------------------------------------|----------------------------------|---|--|-----------------------------------|--------------------------------|
|                       | W <sub>p</sub>                      | Γ <sub>p</sub>                   | W <sub>p</sub>                              | Γ <sub>p</sub>                             | W <sub>p</sub>                    | Γ <sub>p</sub>                 |
| D <sub>13</sub> (3,3) | 1516<br><small>(1510, 1515)</small> | 123<br><small>(115, 110)</small> | not seen<br><small>(1680, not seen)</small> | not seen<br><small>(100, not seen)</small> | 1834<br><small>(1880±100)</small> | 210<br><small>(160±80)</small> |
| D <sub>33</sub> (2,2) | 1609<br><small>(1660, 1655)</small> | 133<br><small>(200, 242)</small> | 2070<br><small>(1900±100)</small>           | 267<br><small>(200±60)</small>             |                                   |                                |
| D <sub>15</sub> (2,2) | 1657<br><small>(1660, 1663)</small> | 132<br><small>(140, 152)</small> | 2188<br><small>(2100±60)</small>            | 238<br><small>(360±80)</small>             |                                   |                                |
| D <sub>35</sub> (2,1) | 1992<br><small>(1890, 1913)</small> | 270<br><small>(250, 246)</small> | not seen<br><small>(2400±60)</small>        | not seen<br><small>(400±150)</small>       |                                   |                                |
| F <sub>15</sub> (2,2) | 1663<br><small>(1670, 1670)</small> | 115<br><small>(120, 120)</small> | 1931<br><small>(not listed)</small>         | 62<br><small>(not listed)</small>          |                                   |                                |
| F <sub>35</sub> (2,2) | 1771<br><small>(1830, 1832)</small> | 190<br><small>(280, 254)</small> | 2218<br><small>(2150±100, 1697)</small>     | 219<br><small>(350±100, 112)</small>       |                                   |                                |
| F <sub>37</sub> (2,1) | 1860<br><small>(1885, 1880)</small> | 201<br><small>(240, 236)</small> | 2207<br><small>(2350±100)</small>           | 439<br><small>(260±100)</small>            |                                   |                                |

Red □ PDG04

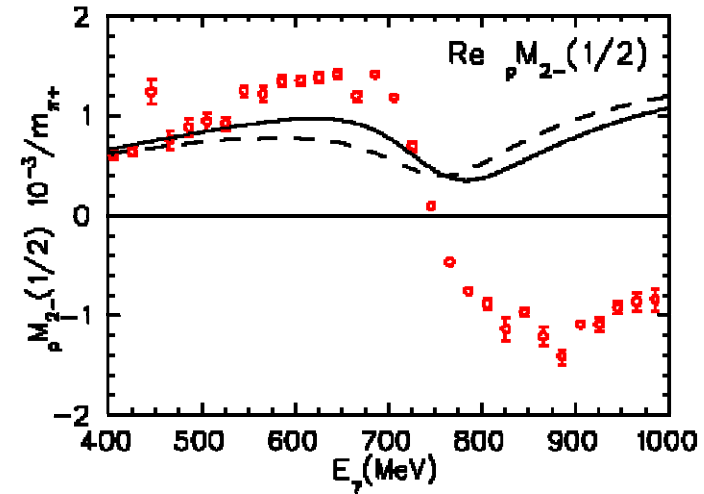
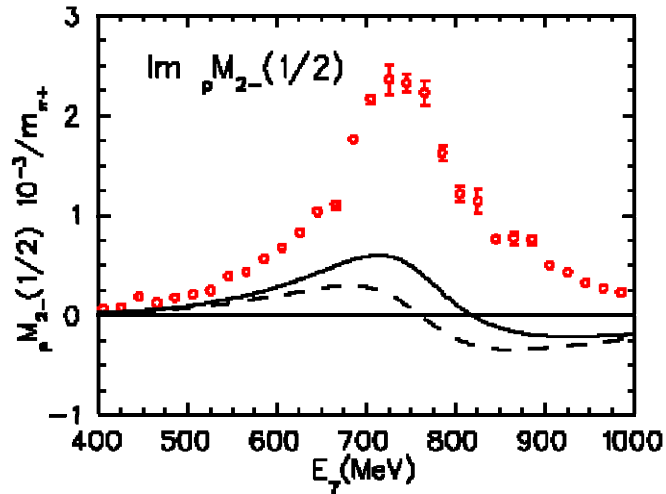
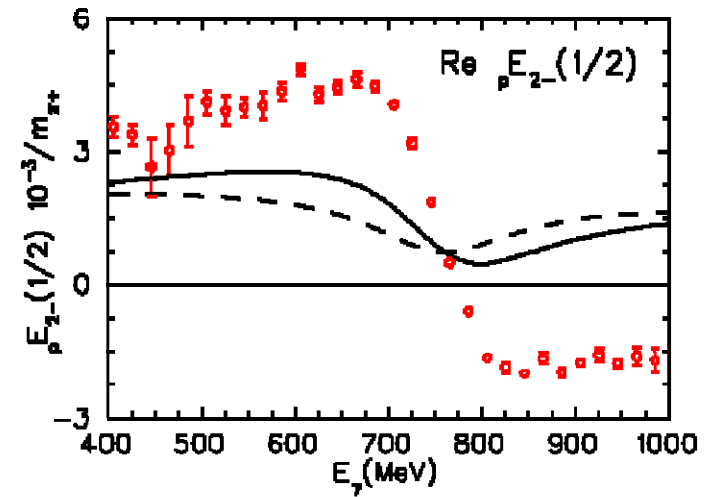
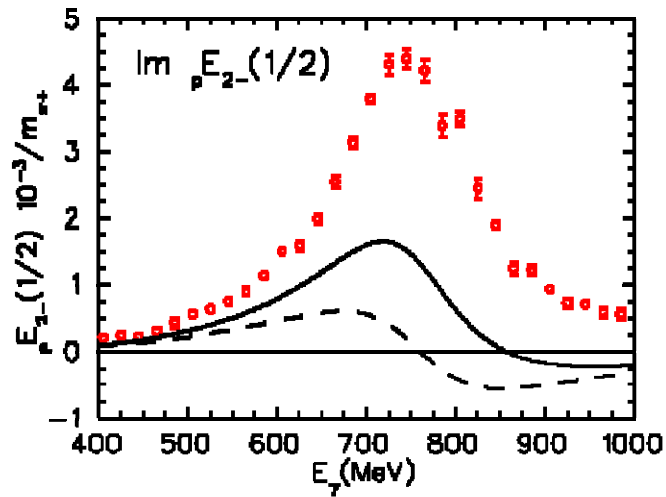
Blue □ Arndt95

Green □ Cutkovsky80

Orange □ Vrana00

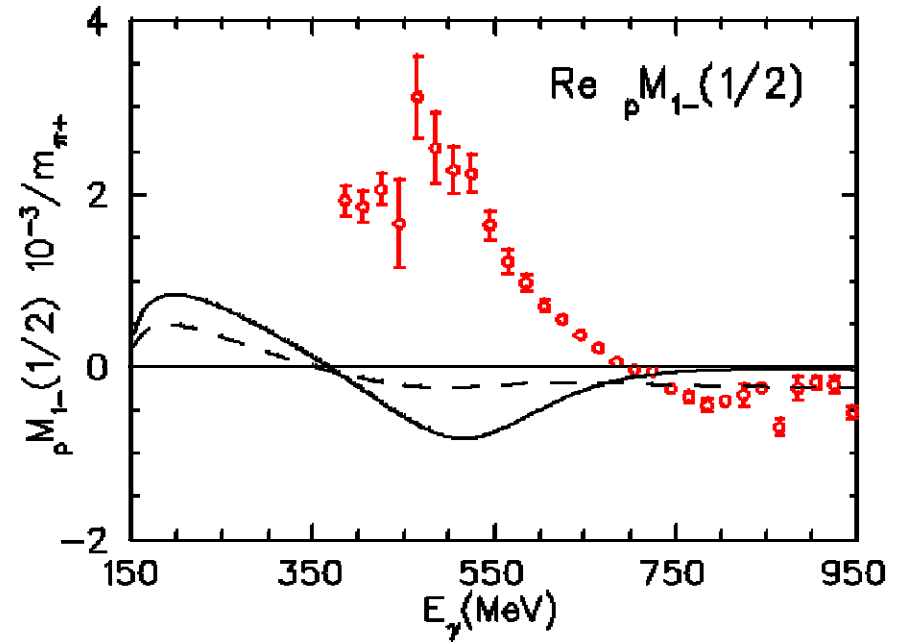
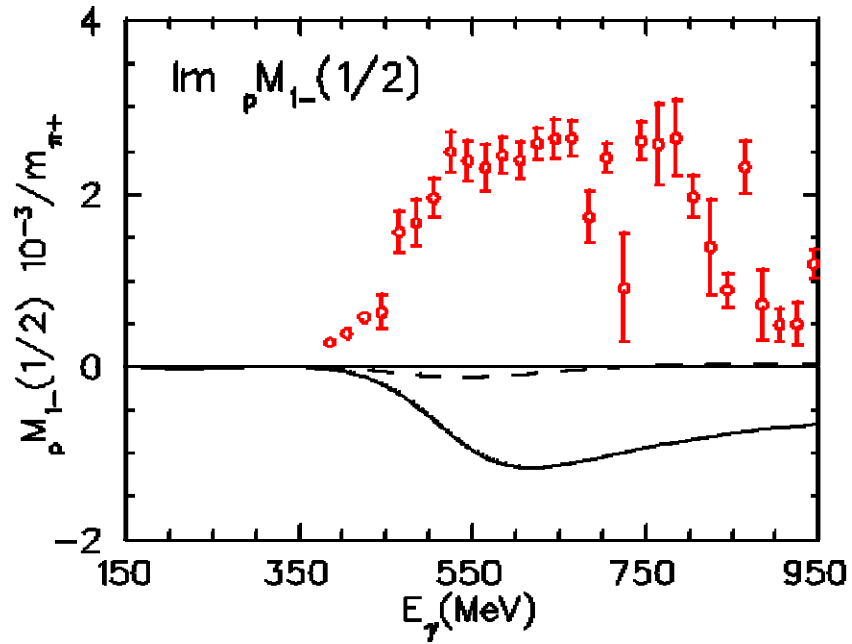
# pion cloud effects:

$D_{13}$

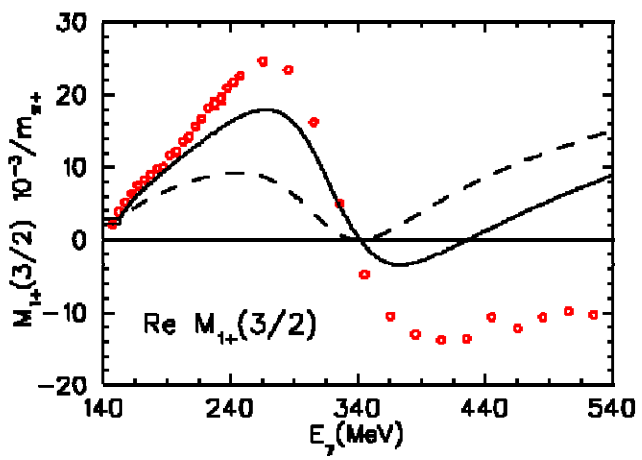
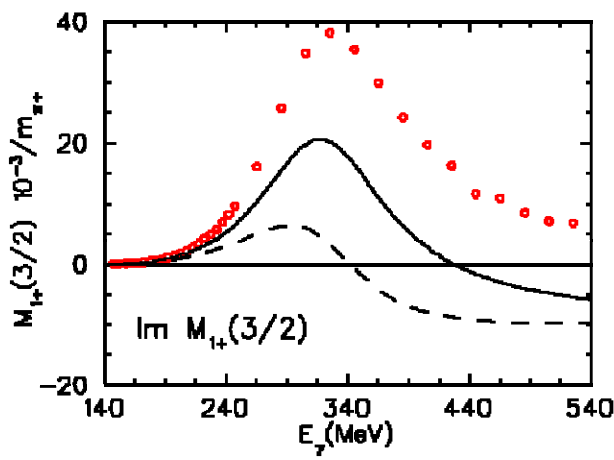
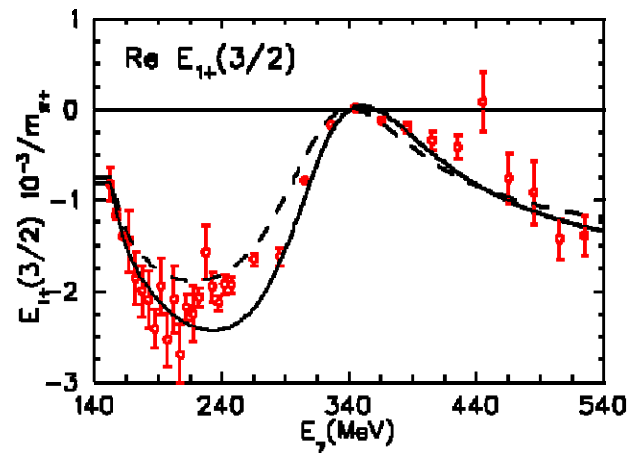
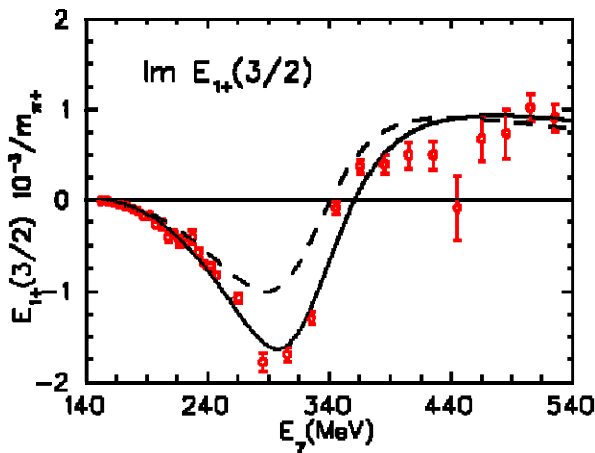


Dashed lines: K-matrix, solid lines: K-matrix + pion clouds

# $P_{11}$

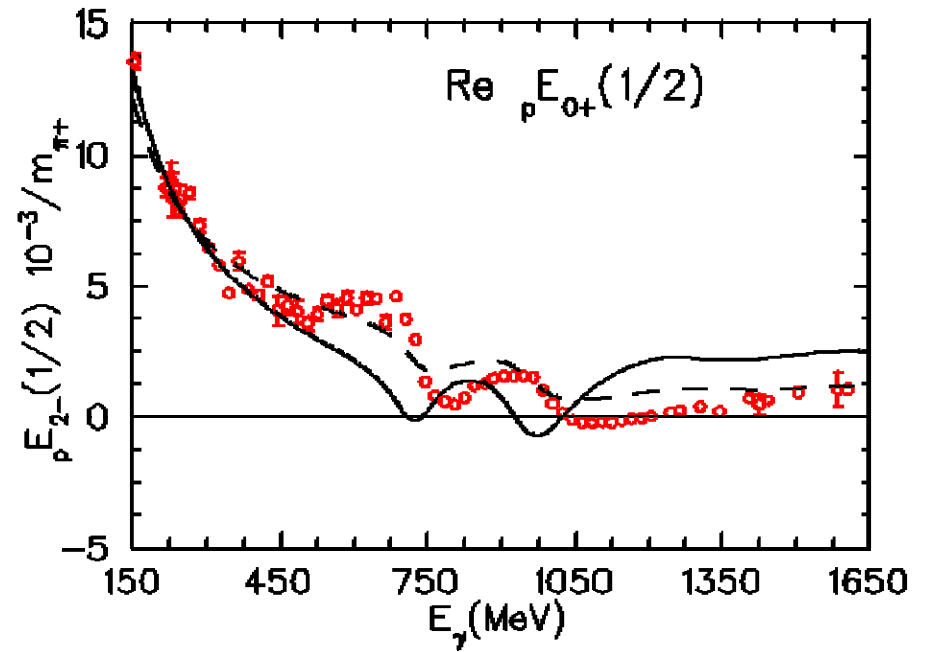
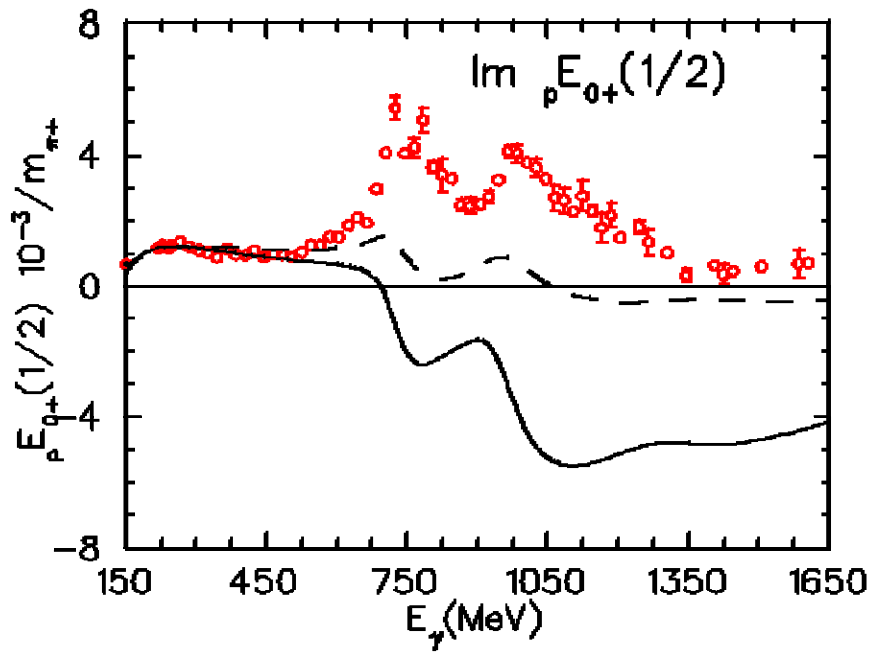


# P<sub>33</sub>





# $S_{11}$



# Summary

- The DMT coupled-channel dynamical model gives excellent description of the pion scattering and pion e.m. production data from threshold to first resonance region
  - Excellent agreement with  $\pi^0$  threshold production data. Two-loop contributions small. For electroproduction, ChPT needs to go at least to  $O(p^4)$ .
  - DMT predicts  $\mu_{N|\Delta} = 3.514 \mu_N$ ,  $Q_{N|\Delta} = -0.081 \text{ fm}^2$ , and  $R_{EM} = -2.4\%$ , all in close agreement with the experiments.  
⇒ dressed  $\Delta$  is **oblate**
  - Bare  $\Delta$  is almost spherical. The oblate deformation of the dressed  $\Delta$  arises almost exclusively from pion cloud

➤ We have re-analyzed the recent Jlab data for the electroproduction of the  $\Delta(1232)$  via  $p(e,e'p)\pi^0$  with DMT and MAID. In contrast with the previous findings, we find

- At  $Q^2=4.0 \text{ (GeV/c)}^2$ , hadronic helicity conservation is still not yet observed.
- $R_{EM}$ , starting from a small and negative value at the real photon point, actually exhibits a clear tendency to cross zero and change sign as  $Q^2$  increases.
- $S_{1/2}$  and  $A_{1/2}$ , but not  $A_{3/2}$ , start exhibiting scaling behavior at about  $Q^2 > 2.5 \text{ (GeV/c)}^2$ .

➡ the onset of scaling might take place at a lower momentum transfer than that of hadronic helicity conservation.

## ➤ Extension to 2.2 GeV gives (preliminary)

- Even pole positions and the number of resonance could be sensitive w.r.t. different analysis tools.
- The pion cloud effects for the pion photoproduction are, in general important, in many channels.

## ➤ Work in progress (completely dynamical)

- extraction of dressed masses, widths,  $Q^2$  evolution of helicity amplitudes ( $\gamma\pi$ )

## ➤ Further theoretical improvements

- Consistent treatment for  $\pi N$  and  $\gamma\pi$
- Gauge invariance
- Sensitivity w.r.t. the  $\pi N$  interaction model
- Effects of other channels like  $\rho N$ ,  $\pi\Delta$ ,  $\sigma N$  et. al.